HHS Public Access

Author manuscript

J Mater Sci Mater Med. Author manuscript; available in PMC 2017 February 09.

Published in final edited form as:

J Mater Sci Mater Med. 2016 July ; 27(7): 121. doi:10.1007/s10856-016-5734-1.

Microsphere-Based Scaffolds Encapsulating Tricalcium Phosphate And Hydroxyapatite For Bone Regeneration

Vineet Gupta[1], **Dina V. Lyne**[2], **Marilyn Barragan**[3], **Cory J. Berkland**[2,4], and **Michael S. Detamore**[1,2]

[1]Bioengineering Graduate Program, University of Kansas, Lawrence, Kansas

[2]Department of Chemical and Petroleum Engineering, University of Kansas, Lawrence, Kansas

[3]Department of Molecular Biosciences, University of Kansas, Lawrence, Kansas

[4]Department of Pharmaceutical Chemistry, University of Kansas, Lawrence, Kansas

Abstract

Bioceramic mixtures of tricalcium phosphate (TCP) and hydroxyapatite (HAp) are widely used for bone regeneration because of their excellent cytocompatibility, osteoconduction, and osteoinduction. Therefore, we hypothesized that incorporation of a mixture of TCP and HAp in microsphere-based scaffolds would enhance osteogenesis of rat bone marrow stromal cells (rBMSCs) compared to a positive control of scaffolds with encapsulated bone-morphogenic protein-2 (BMP-2). Poly(D,L-lactic-co-glycolic acid) (PLGA) microsphere-based scaffolds encapsulating TCP and HAp mixtures in two different ratios (7:3 and 1:1) were fabricated with the same net ceramic content (30 wt%) to evaluate how incorporation of these ceramic mixtures would affect the osteogenesis in rBMSCs. Encapsulation of TCP/HAp mixtures impacted microsphere morphologies and the compressive moduli of the scaffolds. Additionally, TCP/HAp mixtures enhanced the end-point secretion of extracellular matrix (ECM) components relevant to bone tissue compared to the “blank” (PLGA-only) microsphere-based scaffolds as evidenced by the biochemical, gene expression, histology, and immunohistochemical characterization. Moreover, the TCP/HAp mixture groups even surpassed the BMP-2 positive control group in some instances in terms of matrix synthesis and gene expression. Lastly, gene expression data suggested that the rBMSCs responded differently to different TCP/HAp ratios presented to them. Altogether, it can be concluded that TCP/HAp mixtures stimulated the differentiation of rBMSCs toward an osteoblastic phenotype, and therefore may be beneficial in gradient microsphere-based scaffolds for osteochondral regeneration.

Keywords

Tricalcium phosphate; hydroxyapatite; biphasic calcium phosphates; microsphere-based scaffolds; bone regeneration

Address of corresponding author: Michael S. Detamore, Ph.D., Professor, Department of Chemical and Petroleum Engineering, The University of Kansas, 4149 Learned Hall, 1530 W. 15th Street, Lawrence, KS 66045-7618, Phone: (785) 864-4943, FAX: (785) 864-4967, detamore@ku.edu.

1. Introduction

Several regenerative medicine strategies for osteochondral repair have relied on the use of bioceramics such as tricalcium phosphate (TCP) and hydroxyapatite (HAp) for regenerating the bone region of the tissue [1–6].TCP and HAp are both chemically similar to the inorganic component of bone and are osteoconductive because of their capability to bond with bone. TCP lacks osteoinductivity, while HAp is widely accepted to be osteoinductive [7, 8]. On the other hand, HAp degrades over the course of several years, whereas TCP may be resorbed into the new bone tissue [9, 10]. Numerous studies have shown that mixtures of TCP and HAp without the addition of any growth factors or cells can treat large bone defects, which supports their great clinical potential [11–13].

Microsphere-based scaffolds are promising substrates for musculoskeletal regeneration because of their structural attributes like rigidity in shape, ability to provide a porous network, and uniform mechanical properties [14]. Moreover, they offer a wide range of alternatives in terms of materials for microsphere matrices, and methods for microsphere fabrication and sintering [15–20]. Our group has demonstrated that microsphere-based scaffolds can provide opposing signal gradients via spatio-temporal release of growth factors to facilitate regeneration of complex tissues such as the osteochondral interface [21–26]. Furthermore, we have shown that opposing gradients of materials such as TCP and chondroitin sulfate can provide raw materials (i.e., bioactive signals and building blocks) to simultaneously guide the regional osteo- and chondrogenic differentiation of cells [27, 28]. Delivering raw materials in lieu of growth factors holds tremendous financial incentive for translation to the clinic by providing a more streamlined path for regulatory approval as well as saving on the cost of including the growth factor in the product. With regard to osteochondral regeneration, the ceramic mixtures can be combined with chondrogenic raw materials in a gradient scaffold to regenerate the bone region of the tissue. To first evaluate the osteogenic response, the systematic approach is to assess the performance of homogenous microsphere-based scaffolds encapsulating bioceramic mixtures before employing them in a continuously graded design. Therefore, the objective of the current study was to investigate the *in vitro* response of homogenous microsphere-based scaffolds encapsulating TCP and HAp mixtures.

In the current study, we investigated whether encapsulation of a bioceramic mixture (TCP and HAp) in PLGA microsphere-based homogenous scaffolds would promote osteogenesis in rat bone marrow stromal cells (rBMSCs). Homogenous microsphere-based scaffolds were fabricated using PLGA microspheres encapsulating TCP and HAp mixtures in two of the most widely studied w/w ratios of 7:3 and 1:1 (TCP:HAp) with the same net ceramic content of 30 wt% [29–31]. The response of rBMSCs to the bioceramic mixtures was evaluated when cultured in a medium consisting of exogenous factors. Cell response to an osteogenic growth factor, bone morphogenetic protein (BMP)-2, encapsulated in microspheres has been studied in detail in our earlier work [22, 24]. Microsphere-based scaffolds with encapsulated BMP-2 served as the positive control, and “blank” microsphere-based scaffolds (i.e., no BMP-2, TCP or HAp) served as the negative control. We hypothesized that the bioceramic mixture encapsulating groups would outperform the BMP-2 group (positive control) in gene expression and extracellular matrix (ECM) synthesis relevant to bone tissue.

2. Materials and Methods

2.1 Materials

Poly(D,L-lactide-co-glycolide) (PLGA) (50:50 lactic acid:glycolic acid ratio, ester end group) with an intrinsic viscosity (i.v.) of 0.37 dL/g, was obtained from Evonik Industries (Essen, Germany). Human BMP-2 and Murine insulin-like growth factor (IGF)-I were obtained from PeproTech, Inc. (Rocky Hill, NJ). HAp and TCP powders (< 200 nm particle) were obtained from Sigma Aldrich (St. Louis, MO). All other reagents and organic solvents utilized were of cell culture or ACS grade.

2.2 Preparation of Microspheres

Four different types of microspheres were fabricated for the study: - (i) PLGA microspheres (BLANK), (ii) BMP-2 encapsulated PLGA microspheres (BMP), (iii) 7:3 w/w TCP:HAp-encapsulated in PLGA microspheres (abbreviated as TH73 or TCP/HAp 7:3), and (iv) 1:1 w/w TCP:HAp-encapsulated in PLGA microspheres (abbreviated TH11 or TCP/HAp 1:1). For fabricating BMP-2 encapsulated microspheres, BMP-2 was first reconstituted in 10 mg/ml bovine serum albumin (BSA) in phosphate buffered saline (PBS) (both from Sigma, St. Louis, MO). The reconstituted protein solution was mixed with 20% w/v PLGA dissolved in dichloromethane (DCM) at a loading of 60 ng BMP-2 per 1.0 mg of PLGA. The final mixture was then sonicated over ice (50% amplitude, 20 s). The TCP/HAp 7:3 and TCP/HAp 1:1 encapsulated microspheres were fabricated by adding 4.2% and 3% w/v TCP and 1.8% and 3% w/v HAp, respectively to 14% w/v PLGA dissolved in DCM. The net ceramic content encapsulated in TCP/HAp 7:3 and TCP/HAp 1:1 groups was 30 wt%. Using the PLGA-protein and PLGA-TCP/HAp emulsions, microspheres with mean diameters ranging from 172–186 μm (Supplementary Figure 1), were fabricated via our previously reported technology [32, 21, 33, 22, 23, 27, 34, 24, 35, 28, 25, 26, 36–38]. Briefly, using acoustic excitation produced by an ultrasonic transducer (Branson Ultrasonics, Danbury, CT), regular jet instabilities were created in the polymer stream, thereby creating uniform polymer droplets. An annular carrier non-solvent stream of 0.5% w/v poly (vinyl alcohol) (PVA, 88% hydrolyzed, 25 kDa, Polysciences, Inc., Warrington, PA) in deionized water (DI H_2O) carried the emanated polymer droplets (i.e., microspheres) into a beaker containing the non-solvent solution at 0.5% w/v in DI H_2O. The microspheres were stirred for 2–3 h to allow the solvent to evaporate, and then these microspheres were filtered, rinsed and stored at −20°C. The microspheres were then lyophilized for 48 h before further use.

2.3 Scaffold Fabrication

Scaffolds were prepared from the microspheres using our previously established technology [33, 22, 27, 35, 37, 38]. In brief, lyophilized microspheres (50–70 mg) were dispersed in DI H_2O and loaded into a syringe. The dispersion was then pumped using a programmable syringe pump (PHD 22/2000; Harvard Apparatus, Inc., Holliston, MA) into a cylindrical plastic mold (diameter ~ 4 mm) having a filter at the bottom until a height of about 2 mm was reached. The scaffolds were 3.8–4.0 mm in diameter and around 2 mm in height. The packed microspheres were then sintered with ethanol-acetone (95:5 v/v) for 55 min. The scaffolds were further lyophilized for 48 h and sterilized with ethylene oxide for 12 h prior to cell seeding experiments. A total of four different groups were tested in the study and

were named according to the composition of microspheres as: BLANK, BMP, TH73 or TCP/HAp 7:3, and TH11 or TCP/HAp 1:1.

2.4 Cell Seeding of Scaffolds

rBMSCs were obtained from the femurs of eight young male Sprague–Dawley rats (176–200 g, SASCO) following a University of Kansas approved IACUC protocol (175–08) and cultured in medium consisting of αMEM supplemented with 10% FBS (MSC-Qualified, cat #10437-028) and 1% penicillin–streptomycin (P/S) (both from Thermofisher Scientific, Waltham, MA). When the cells were 80% to 90% confluent, they were trypsinized and re-plated at 7,500 cells/cm^2. Seeding was performed when cells reached P4. Scaffolds were sterilized using ethylene oxide for 12 h, allowed to ventilate overnight after sterilization, and placed in a 48-well plate. Cells (P4) were resuspended in culture medium at a concentration of approximately 50 million/mL. 25 μL of this cell suspension (~1.25M cells) was placed directly onto the top of the scaffold, which infiltrated the scaffold via capillary action [33, 27]. Cells were allowed to attach for 1 h, after which 1 mL of culture medium was added. After 24 h, the culture medium was replaced by 1 mL of differentiation medium consisting of αMEM, 1% P/S, 10% FBS, 4 mM β-glycerophosphate (β-GP), 100 nM dexamethasone (DEX) (MP Biomedicals, Santa Ana, CA), 1% insulin-transferrin-selenium 100X (ITS) (Thermofisher Scientific, Waltham, MA), 1% non-essential amino acids (NEAA) (Thermofisher Scientific, Waltham, MA), 15 mM HEPES buffer (Thermofisher Scientific, Waltham, MA), and 100 ng/mL murine IGF-I. Every 48 h for 6 weeks, three-fourths of the differentiation medium was replaced with fresh medium.

2.5 Scanning Electron Microscopy (SEM) and Energy Dispersion Spectroscopy (EDS)

Microspheres and acellular scaffolds were imaged via a Versa 3D Dual Beam (FEI, Hillsboro, OR) scanning electron microscope (SEM) with a detector for energy dispersive spectroscopy (EDS). The BMP and TH11 microspheres were cryo-fractured using a sharp blade and the dispersion of BMP-2, TCP and HAp within the microspheres was further analyzed using EDS at an accelerating voltage of 10 kV. Pixel maps for atomic calcium, nitrogen and phosphorus were generated using Aztec analysis software (Oxford Instruments, Abingdon, United Kingdom). The PLGA (BLANK) microspheres were also imaged as a negative control to confirm the absence of calcium, nitrogen and phosphorous in the EDS maps.

2.6 Mechanical Testing

Unconfined compression tests of acellular (i.e., week 0) microsphere-based scaffolds (n = 6) were conducted using a uniaxial testing apparatus (Instron Model 5848, Canton, MA) with a 50 N load cell. A custom-made stainless steel bath and a compression-plate assembly were mounted in the apparatus [39]. Cylindrical scaffold samples were compressed to 40% strain at a strain rate of 10%/min under phosphate-buffered saline [PBS—0.138 M sodium chloride, 0.0027 M potassium chloride] at 37°C. Among all possible testing modalities, compression at a 10%/min strain rate provides the most valuable information in terms of achieving high strain levels to view the entire stress-strain profile, which cyclic testing and stress relaxation/creep testing do not provide, and moreover a reproducible elastic modulus can be obtained without preconditioning as we have done in the past [40]. Compressive

moduli of elasticity were calculated from the initial linear regions, i.e., at ~5% strain, of the stress-strain curves as described previously [33, 27, 35, 26, 37, 38].

2.7 Porosity Measurement

We have previously demonstrated a close match between theoretical porosities and porosities measured by porosimetry and microCT [34, 26]. Therefore, a fluid saturation method as described previously [27] was used in this study to calculate the porosities of the scaffolds:

$$V\_B = 4m \div \pi d\hat{}2h,$$

$$W\_\text{Water} = W\_W - W\_D,$$

$$V\_P = W\_\text{Water} \div \rho\_\text{Water},$$

$$\text{Porosity}(\varphi)(\%) = (V\_P \div V\_B) \times 100\%$$

where V_B, m, d, h, W_W, W_D, V_P are the bulk volume, mass, diameter, height, wet weight, dry weight, and pore volume of the scaffolds, respectively. W_{Water} and ρ_{Water} are the weight and density of water. Briefly, wet and dry weights of scaffolds were recorded after fabrication and porosities were determined by the above-described method.

2.8 Biochemical Analyses

Engineered constructs were analyzed for matrix production at 0 (i.e., 24 h post seeding), 3, and 6 weeks. The samples were digested in two different types of digestion solution (n = 6 for each): (i) Papain solution for DNA and hydroxyproline (HYP) content analyses, and (ii) Triton-X solution for calcium content and ALP activity analyses. The papain digestion solution consisted of 125 mg/mL papain (from papaya latex), 5 mM N-acetyl cysteine, 5 mM ethylenediaminetetraacetic acid, and 100 mM potassium phosphate buffer (20 mM monobasic potassium phosphate, 79 mM dibasic potassium phosphate) (all reagents from Sigma Aldrich) in DI H_2O. Engineered constructs were removed from culture in a sterile manner, placed in microcentrifuge tubes, homogenized with the papain solution (1 mL), and allowed to digest overnight in a 60°C water bath. The digested scaffolds were then centrifuged at 10,000 rpm for 5 minutes to pellet fragments of polymer and other impurities and stored at −20°C. Later, the supernatant was used to determine DNA and hydroxyproline (HYP) contents using the PicoGreen (Molecular Probes, Eugene, OR) and HYP (cat #MAK008, Sigma Aldrich, St. Louis, MO) assays, respectively. For calcium and ALP analyses, constructs were digested in 0.05% Triton X-100 (Sigma Aldrich, St. Louis, MO) and the supernatants were stored at −20°C before the analyses. Calcium content and alkaline phosphatase (ALP) activity were assessed using the QuantiChromTM Calcium Assay (DICA-500; QuantiChrom, Hayward, CA) and Alkaline Phosphatase Activity Colorimetric

Assay (K412–500, Biovision, Milpitas, CA) kits, respectively. The calcium contents of the acellular controls for TCP/HAp 7:3 and TCP/HAp 1:1 groups were also measured at each time point in an effort to distinguish the bioactivity provided by TCP and HAp from the calcium amounts retained in the scaffolds. The calcium contents for the TCP/HAp 7:3 and TCP/HAp 1:1 groups (both cellular and acellular) at week 0 are not reported because of incomplete extraction of calcium from these scaffolds.

2.9 Gene Expression Analyses

Reverse transcriptase quantitative polymerase chain reaction (RT-qPCR) was performed for gene expression analyses in microsphere-based constructs (n = 6) at weeks 0, 1.5, 3, and 6. Certain groups at certain time points (indicated in Results section) had no Ct values, indicating that the fluorescence intensities in these samples did not cross the threshold fluorescence. These samples were marked as zero for RNA expression. RNA was isolated and purified using QIAshredders and an RNeasy Kit (Qiagen, Valencia, CA) according to the manufacturer's guidelines. Isolated RNA was converted to complementary DNA using a TaqMan High Capacity kit (Applied Biosystems, Foster City, CA) in an Eppendorf RealPlex Mastercycler. TaqMan Gene expression assays from Applied Biosystems for appropriate genes (Table 1) were run in the Eppendorf system. A $2^{-\Delta\Delta Ct}$ method was used to evaluate the relative level of expression for each target gene. For quantification, the BLANK constructs at week 0 were designated as the calibrator group and GAPDH expression as the endogenous control.

2.10 Histology and Immunohistochemistry (IHC)

At 6 weeks, microsphere-based constructs (n = 3) were soaked in 30% w/v sucrose (Thermofisher Scientific, Waltham, MA) solution in PBS for 24 h. Afterward, the constructs were equilibrated in optimal cutting temperature embedding medium (OCT, Tissue-Tek, Torrance, CA) overnight at 37°C and then frozen at −20°C. 10 μm thick sections were cut using a cryostat (Micron HM-550 OMP, Vista, CA) and stained using Hematoxylin (cell nuclei) and Eosin (cytoplasm); Masson's trichrome for collagen, cell nuclei, and cytoplasm; Alizarin red for calcium phosphates; von Kossa for mineralization; and Sudan Black for residual polymer. Acellular constructs (n = 2) at week 6 from the TCP/HAp 7:3 and TCP/HAp 1:1 groups were also stained using Alizarin red and von Kossa. The sections from cellular constructs were stained for the presence of collagen type I using immunohistochemistry (IHC). Mouse monoclonal anti-collagen type I (1:200 dilution; Thermofisher Scientific, Waltham, MA) primary antibody was used for the immunostaining. Following the primary antibody, biotinylated secondary antibody was used followed with the ABC complex (Vector Laboratories, Burlingame, CA). The antibodies were visualized with the diaminobenzidine (DAB) substrate per the manufacturer's (Vector Laboratories, Burlingame, CA) protocol. Negative controls were also run with the primary antibody omitted.

2.11 Statistical Analyses

GraphPad Prism 6 statistical software (GraphPad Software, Inc., La Jolla, CA) was used to compare experimental groups using a one-factor ANOVA (sections 2.6 and 2.7) or a two-factor ANOVA (sections 2.8 and 2.9) followed by a *Tukey's post hoc* test, where $p < 0.05$

was considered significant. Additionally, standard box plots were constructed to eliminate outliers. All quantitative results are reported as average ± standard deviation within text or as average + standard deviation within figures.

3. Results

3.1 Scanning Electron Microscopy (SEM)

Figure 1 represents the scanning electron micrographs of all four types of microspheres. The microspheres in the BLANK (i.e., PLGA only) group had a smooth surface, while the microspheres in the BMP, TH73 (TCP/HAp 7:3), and TH11 (TCP/HAp 1:1) groups had minute pores on their surfaces. The BLANK and the BMP microspheres had a spherical morphology, whereas the TH73 and TH11 microspheres had a deflated soccer ball-like appearance with obvious indentations on the surfaces of the microspheres. Figure 2 depicts the distribution of atomic calcium (Ca), nitrogen (N) and phosphorous (P) in the interior of BLANK, BMP, and TH11 microspheres. As expected, the three elements were essentially absent from the BLANK microspheres. Nitrogen was uniformly distributed inside the BMP microspheres as demonstrated by the spectral maps. The EDS maps also depicted the presence of phosphorus and calcium in the BMP microspheres. Calcium and phosphorous were uniformly distributed inside the TH11 microspheres, while nitrogen was absent from the TCP/HAp 1:1 group. Figure 3 represents the SEM images of all of the scaffold groups used for the study. All scaffolds were porous in nature with interconnected pores.

3.2 Mechanical Testing

BLANK scaffolds had an average compressive modulus of 330 ± 120 kPa that was 80% ($p < 0.05$) and 40-fold ($p < 0.05$) higher than the moduli of TCP/HAp 7:3 and TCP/HAp 1:1 scaffolds, respectively (Figure 4). The average moduli of the BMP and TCP/HAp 7:3 groups were 35-fold ($p < 0.05$) and 22-fold ($p < 0.05$) higher than the modulus of the TCP/HAp 1:1 group, respectively. No significant differences in compressive modulus were observed between the BMP and TCP/HAp 7:3 groups, or between the BMP and BLANK groups.

3.3 Porosity Measurement

The average porosity of the TCP/HAp 1:1 group was 47.7 ± 5.0%, which was 1.9-fold ($p < 0.05$), 1.5-fold ($p < 0.05$), and 1.3-fold ($p < 0.05$) higher than the porosities of the BLANK, BMP, and TCP/HAp 7:3 groups, respectively (Figure 5). The porosity of the TCP/HAp 7:3 group was 1.5-fold ($p < 0.05$) higher than the porosity of the BLANK group. No significant differences in porosities were observed between the BLANK and BMP groups.

3.4 Biochemical Analysis

3.4.1 DNA content—At week 0, the BLANK group had 8.3-fold ($p < 0.05$) and 3.1-fold ($p < 0.05$) higher DNA content than the TCP/HAp 7:3 and TCP/HAp 1:1 groups, respectively (Figure 6). The DNA content of the BMP group at week 0 was 7.2-fold ($p < 0.05$) and 2.7-fold ($p < 0.05$) higher than the DNA contents of the TCP/HAp 7:3 and TCP/HAp 1:1 groups, respectively. No significant differences in DNA content were observed between the TCP/HAp 7:3 and TCP/HAp 1:1 groups at week 0. Additionally, no significant differences were observed in DNA content among the groups at weeks 3 or 6.

The DNA contents in the BLANK and BMP groups at week 0 were statistically significantly higher than their corresponding values at later time points, while no significant changes in DNA content were observed in the TCP/HAp 7:3 and TCP/HAp 1:1 groups over time. The BLANK group at week 0 had 22-fold ($p < 0.05$) and 8.6-fold ($p < 0.05$) higher amounts of DNA than its values at weeks 3 and 6, respectively. The BMP group at week 0 had 29-fold ($p < 0.05$) and 6-fold ($p < 0.05$) higher DNA content than its corresponding values at weeks 3 and 6, respectively.

3.4.2 Hydroxyproline (HYP) content—At week 0, the BLANK group had 11-fold ($p < 0.05$) higher net HYP content than the BMP group (Figure 7A). No significant differences in net HYP content were observed among any other groups at week 0. Additionally, no significant differences in net HYP content were observed among the groups at week 3. Week 6 net HYP content results showed that only the TCP/HAp 7:3 group outperformed the BLANK control, with HYP content that was 2.7-fold ($p < 0.05$) higher. No significant differences in net HYP content were observed among any other groups at week 6. Only the BMP and TCP/HAp 7:3 groups showed significant changes in net HYP content over time. The BMP group at week 6 had 13-fold ($p < 0.05$) higher net HYP than its corresponding value at week 0. The net HYP contents of the TCP/HAp 7:3 group at weeks 3 and 6 were 9.6-fold ($p < 0.05$) and 15-fold ($p < 0.05$) higher than its HYP content at week 0, respectively. In the normalized HYP (per DNA) content, no significant differences were observed among the groups at weeks 0 and 3 (Figure 7B). At week 6, both the TCP/HAp 7:3 and TCP/HAp 1:1 groups outperformed the BLANK control in normalized HYP content with values that were 14-fold ($p < 0.05$) and 6.9-fold ($p < 0.05$) higher, respectively. Moreover, the normalized HYP contents in the TCP/HAp 7:3 and TCP/HAp 1:1 groups at week 6 were 15-fold ($p < 0.05$) and 7.9-fold ($p < 0.05$) higher than the HYP content in the BMP group, respectively. Additionally, the normalized HYP content in the TCP/HAp 7:3 group at week 6 was 2-fold ($p < 0.05$) higher than the HYP content in the TCP/HAp 1:1 group. Only the TCP/HAp 7:3 and TCP/HAp 1:1 groups showed significant changes in normalized HYP content over time. The TCP/HAp 7:3 group at week 6 had 35-fold ($p < 0.05$) and 3.4-fold ($p < 0.05$) higher normalized HYP content than its matching values at weeks 0 and 3, respectively. The TCP/HAp 1:1 group at week 6 had 6.7-fold ($p < 0.05$) higher normalized HYP content than its value at week 0.

3.4.3 ALP activity—No significant differences were observed in the ALP activities among the groups at weeks 0 and 3 (Figure 8). However, at week 6, the TCP/HAp 7:3 and TCP/HAp 1:1 groups outperformed the BLANK control in ALP activity, with activities that were 40-fold ($p < 0.05$) and 20-fold ($p < 0.05$) higher, respectively. Additionally, the TCP/HAp 7:3 and TCP/HAp 1:1 groups at week 6 surpassed the BMP group in ALP activity, with activities that were 40-fold ($p < 0.05$) and 20-fold ($p < 0.05$) higher, respectively. Also, the ALP activity of the TCP/HAp 7:3 group at week 6 was 2-fold ($p < 0.05$) higher than the ALP activity of the TCP/HAp 1:1 group. Only the TCP/HAp 7:3 showed significant changes in ALP activity over time, with its week 6 activity being 1.8-fold ($p < 0.05$) and 3.3-fold ($p < 0.05$) higher than its activities at weeks 0 and 3, respectively.

3.4.4 Calcium content—The calcium contents for the cellular BLANK and BMP constructs at week 0 were 32.7 ± 5.3 μg and 54 ± 19 μg, respectively. The calcium contents for the TCP/HAp 7:3 and TCP/HAp 1:1 groups (both cellular and acellular) at week 0 are not reported because of inadequate extraction of calcium from these scaffolds at that time point. Week 3 calcium content results showed no significant differences among groups at that time point (Figure 9). At week 6, the calcium content of the BMP group was 1.7-fold ($p < 0.05$) higher than the calcium content of the TCP/HAp 1:1 group. The calcium content of the TCP/HAp 7:3 group at week 6 was 3.3-fold ($p < 0.05$) higher than the calcium content of the TCP/HAp 7:3 [Acellular] group. No significant differences were observed in calcium content among the other groups at week 6. The BLANK group at week 3 had 21-fold ($p < 0.05$) and 1.7-fold ($p < 0.05$) higher calcium content than its corresponding values at weeks 0 and 6, respectively. Additionally, the calcium content of the BLANK group at week 6 was 12-fold ($p < 0.05$) higher than its calcium content at week 0. The BMP group at weeks 3 and 6 had 12-fold ($p < 0.05$) and 10-fold ($p < 0.05$) higher calcium contents than its matching value at week 0, respectively. The calcium content of the TCP/HAp 1:1 group at week 3 was 1.7-fold ($p < 0.05$) higher than its corresponding value at week 6. The TCP/HAp 7:3 [Acellular] and TCP/HAp 1:1 [Acellular] groups at week 3 had 3.9-fold ($p < 0.05$) and 3.2-fold ($p < 0.05$) higher amounts of calcium than their matching values at week 6, respectively. No other group showed statistically significant changes in calcium content over time.

3.5 Gene Expression

3.5.1 RUNX2 and COL1A1—Both the BLANK and the BMP groups at week 0 had 3-fold ($p < 0.05$) higher relative RUNX2 expression than the expression of the TCP/HAp 7:3 group (Figure 10A). No significant differences were observed in the RUNX2 expression at week 0 among the BLANK, BMP and TCP/HAp 1:1 groups. At week 1.5, the RUNX2 expression for the TCP/HAP 7:3 group was 2.1-fold ($p < 0.05$) and 3.8-fold ($p < 0.05$) higher than the expression values for the BMP and TCP/HAp 1:1 groups, respectively. No significant differences in RUNX2 expression were observed among the groups at weeks 3 and 6. The TCP/HAp 7:3 and TCP/HAp 1:1 groups were the only groups that showed statistically significant changes in RUNX2 expression over time. The TCP/HAp 7:3 group at week 0 had 7.3-fold ($p < 0.05$) higher expression than at week 6. At week 1.5, the TCP/HAp 7:3 group had 4.2-fold ($p < 0.05$) and 31-fold ($p < 0.05$) higher RUNX2 expression than its matching values at weeks 0 and 6, respectively. Moreover, the TCP/HAp 7:3 group at week 3 had 18-fold ($p < 0.05$) higher RUNX2 expression than its expression at week 6. The TCP/HAP 1:1 group at week 3 had 3.7-fold ($p < 0.05$), 4.3-fold ($p < 0.05$), and 2.8-fold ($p < 0.05$) higher RUNX 2 expression than its expression values at weeks 0, 1.5, and 6, respectively.

The COL1A1 (collagen I) expression values (Figure 10B) of the BLANK, BMP, and TCP/HAp 1:1 groups at week 0 were 2-fold ($p < 0.05$), 2-fold ($p < 0.05$), and 1.7-fold ($p < 0.05$) higher than the expression value of the TCP/HAp 7:3 group, respectively. No significant differences were observed in COL1A1 expression among the BLANK, BMP, and TCP/HAp 1:1 groups at week 0. Additionally, no significant differences were observed in COL1A1 expression among the groups at weeks 1.5 and 3. At week 6, the TCP/HAP 1:1 group outperformed the BLANK and BMP controls in COL1A1 expression with 7.5-fold (p

< 0.05) and 15-fold ($p < 0.05$) higher expression, respectively. In addition, the TCP/HAp 1:1 group at week 6 had 60-fold ($p < 0.05$) higher COL1A1 expression than the TCP/HAp 7:3 group at that time point. All of the groups showed statistically significant changes in COL1A1 expression over time. The BLANK group at week 0 had 5.4-fold ($p < 0.05$), 9.8-fold ($p < 0.05$), and 12-fold ($p < 0.05$) higher COL1A1 expression than its corresponding values at weeks 1.5, 3, and 6, respectively. The BMP group at week 0 had 7.4-fold ($p < 0.05$), 11-fold ($p < 0.05$), and 24-fold ($p < 0.05$) higher COL1A1 expression than its matching values at weeks 1.5, 3, and 6, respectively. The COL1A1 expression values of the TCP/HAp 7:3 group at weeks 0 and 1.5 were 48-fold ($p < 0.05$) and 34-fold ($p < 0.05$) higher than its week 6 value, respectively. The TCP/HAp 1:1 group at week 0 had 3.8-fold ($p < 0.05$) and 2.1-fold ($p < 0.05$) higher COL1A1 expression than its corresponding expression at weeks 1.5 and 3, respectively. Additionally, the TCP/HAp 1:1 group at week 6 had 2.7-fold ($p < 0.05$) higher COL1A1 expression than its matching value at week 1.5.

3.5.2 BGLAP and IBSP—The BGLAP expression values for the BLANK group at weeks 1.5, 3, and 6; BMP group at weeks 1.5 and 3; TCP/HAp 7:3 group at week 3; and TCP/HAp 1:1 group at weeks 1.5 and 3, were marked as zero because the fluorescence intensities in these samples did not cross the threshold fluorescence. BGLAP expression (Figure 10C) showed no significant differences among groups at week 0. At week 1.5, the relative BGLAP expression of the TCP/HAp 7:3 group was statistically significantly ($p < 0.05$) higher than the expression of the BLANK, BMP, and TCP/HAp 1:1 groups. No significant differences were observed in BGLAP expression among the groups at week 3. Week 6 BGLAP expression showed that the BMP group expression was statistically significantly ($p < 0.05$) higher than the expression of the BLANK group. In addition, the BMP group BGLAP expression at week 6 was 74-fold ($p < 0.05$) higher than the expression of the TCP/HAp 7:3 group. No significant differences in BGLAP expression were observed at week 6 between the BMP and TCP/HAp 1:1 groups. Only the BMP and TCP/HAp 7:3 groups showed statistically significant changes in BGLAP expression over time. The BMP group at week 6 had statistically significantly ($p < 0.05$) higher BGLAP expression than its expression values at weeks 1.5 and 3. The TCP/HAp 7:3 group at week 1.5 had 14-fold ($p < 0.05$) and 113-fold ($p < 0.05$) higher BGLAP expression than its corresponding values at weeks 0 and 6. Moreover, the TCP/HAp 7:3 group at weeks 1.5 and 6 had statistically significantly ($p < 0.05$) higher BGLAP expression than its value at week 3.

The IBSP expression values for the BLANK group at weeks 1.5 and 3; BMP group at weeks 3 and 6; TCP/HAp 7:3 group at weeks 1.5, 3, and 6; and TCP/HAp 1:1 group at weeks 1.5 and 3, were marked as zero because the fluorescence intensities in these samples did not cross the threshold fluorescence. No significant differences were observed in IBSP expression among the groups at weeks 0, 1.5 and 3 (Figure 10D). The TCP/HAp 1:1 group at week 6 outperformed the BLANK control with 98-fold ($p < 0.05$) higher IBSP expression. Moreover, the IBSP expression for the TCP/HAp 1:1 group at week 6 was statistically significantly ($p < 0.05$) higher than the expression of the BMP and TCP/HAp 7:3 groups. Only the TCP/HAp 1:1 group showed statistical significant changes in IBSP expression over time. The TCP/HAp 1:1 group at week 6 had 193-fold ($p < 0.05$) higher IBSP expression than its corresponding expression at week 0. Additionally, the TCP/HAp 1:1 group at week 6

had statistically significantly ($p < 0.05$) higher expression than its matching values at weeks 1.5 and 3.

3.6 Histology and Immunohistochemistry

Figure 11 represents the histological staining for the BLANK, BMP, TH73 (TCP/HAp 7:3), and TH11 (TCP/HAp 1:1) groups at week 6. From H&E staining, it was clear that the BLANK and BMP groups were primarily tissue without any evidence of spherical microsphere shapes as observed in the TH73 and TH11 groups. Additionally, H&E images indicated toward higher cell numbers in the BLANK and BMP groups compared to the TCP/HAp groups. Masson's trichrome staining images showed no apparent differences in staining intensities between the BLANK and BMP groups or between the TCP/HAp 7:3 and TCP/HAp 1:1 groups. The TCP/HAp groups had higher numbers of blue stained specks for collagen (indicated by arrows in than those observed in the BLANK and BMP groups. Alizarin red and von Kossa staining for calcium and calcium deposits was observed in all of the groups. The TCP/HAp 7:3 group stained more intensely for calcium and calcium deposits than the TCP/HAp 1:1 group, while no differences in staining intensities were observed between the BLANK and BMP groups. Additionally, the TCP/HAp groups had higher staining intensities for both the Alizarin Red and von Kossa than the staining intensities in the BLANK and BMP groups. The higher staining intensities for Alizarin red and von Kossa in the TCP/HAp scaffolds could be attributed to inherent calcium present in these scaffolds, which was confirmed by the histological images of the acellular TCP/HAp scaffolds (Supplementary Figure 2). All of the groups stained positively for Sudan Black, and microsphere architecture was evident in the TCP/HAp groups, whereas no discernable microsphere shapes were noted in the BLANK and BMP groups. The observance of intact microsphere structure with Sudan Black staining suggest that TCP and HAp encapsulation might have altered polymer degradation, which was also indicated by the macroscopic observations where the culture medium in the acellular BLANK and BMP scaffolds became acidic more rapidly than the medium in their TCP/HAp counterparts (Supplementary Figure 3). Immunohistochemical (IHC) staining of week 6 microsphere-based scaffolds was positive for collagen I (Figure 12). Collagen I staining was more intense in the TCP/HAp 1:1 group than the staining in the BLANK and TCP/HAp 7:3 groups. Moreover, the BMP group had more intense staining for collagen I than the staining in the BLANK group.

4. Discussion

The current study was the first to examine the effects of encapsulating TCP and HAp mixtures for stimulating osteogenesis in microsphere-based scaffolds. This work builds on our previous efforts establishing that incorporation of inorganic materials such as TCP, HAp, and bioactive glass (BG) alone in microsphere-based scaffolds provides both bioactive cues and building blocks for osteogenic differentiation of cells [33, 27, 24, 35, 28]. Additionally, it has been shown by others that combining TCP and HAp for bone regeneration is a promising strategy given that a combination of these materials provides both osteoinductive and osteoconductive cues to the surrounding cells [30, 41, 42, 31, 43–46]. Furthermore, we have previously demonstrated that higher concentrations (10 and 20 wt%) of TCP and HAp in microsphere-based scaffolds were more favorable for synthesis of ECM components

relevant to bone tissue, thus providing the motivation for encapsulating even higher concentrations of TCP and HAp than our previous reported studies [33, 27]. Hence, the present study investigated the response of rBMSCs to TCP/HAp mixtures, encapsulated at a concentration of 30 wt%, during osteogenic differentiation on microsphere-based scaffolds.

The SEM images depicted that all four types of microspheres were uniform in size, with average microsphere diameter ranging between 172–186 μm (Supplementary Figure 1). The BMP, TH73 (TCP/HAP 7:3), and TH11 (TCP/HAp 1:1) microspheres possessed micron and sub-micron pores on their surface, which could be attributed to particulate leaching during solvent removal and droplet hardening process [25]. Additionally, it was observed that the TH73 and TH11 microspheres had a deflated soccer ball-like shape, which may have contributed toward higher average porosities in the TCP/HAp 7:3 and TCP/HAp 1:1 scaffolds compared to the BLANK and BMP groups. The deflated shapes might have resulted from the incongruent solvent exchange across the microsphere surface as a direct consequence of changes in emulsion viscosity due to addition of TCP/HAp mixtures into the polymer phase. We observed a similar phenomenon with PLGA microspheres containing bioactive glass (BG), where these microspheres were spherical in shape at the time of fabrication but lost their shape during the droplet hardening step [35]. Similar to our observations, Bao *et al.* [47] noted that the encapsulation of biphasic calcium phosphates (BCP) at a concentration of 30% or higher in poly(ε-caprolactone) microspheres fabricated using the emulsion solvent-evaporation method, also resulted in irregularly-shaped microspheres. It was suggested that the viscosity of the dispersion mixture of polymer and BCP increased with BCP concentrations higher than 30%, thereby affecting the dispersibility of the microemulsion in the continuous phase and also the efflux velocity of solvent during the solvent exchange that further led to non-uniform shaped microspheres with sunken structures. Although we noticed differences in microsphere morphologies among the groups, the scaffolds in all the groups were found to be porous in nature with interconnections among the pores, which agreed with our previous findings [27, 26]. Furthermore, the elemental distribution of calcium and phosphorus as observed via EDS confirmed the uniform distribution of calcium phosphates inside the TCP/HAp microspheres with no evidence of agglomeration at any site. The BMP microspheres depicted the presence of phosphorus that could be attributed to the PBS buffer used for reconstitution of the protein. The presence of calcium in BMP microspheres could be regarded as artifacts of the automatic peak identification software used for the EDS analysis [48].

Uniaxial compression testing results showed that the compressive moduli of microsphere-based scaffolds were within an order of magnitude of the moduli for cancellous bone [49, 50]. The compressive modulus of BLANK scaffolds was found to be at least 2 times as large as the moduli of the TCP/HAP 7:3 and TCP/HAp 1:1 groups, while the porosities of the TCP/HAp groups were at least 1.5 times larger than the porosity of the BLANK scaffolds. The compressive modulus results agreed with our previous findings that the presence and subsequent modification of microspheres by calcium phosphates led to lower moduli of TCP/HAp scaffolds compared to the BLANK controls [33, 25]. Additionally, the modulus of TCP/HAp 1:1 scaffolds was significantly lower than the moduli of the BMP and TCP/HAp 7:3 groups. The lower modulus in the TCP/HAp 1:1 group may be attributed to its higher

porosity as it has been shown that the compressive modulus is inversely related to the porosity of scaffolds [51, 52].

The biochemical content results revealed some interesting trends. It was observed that the TCP/HAp scaffolds at week 0 (24 h post seeding) had significantly lower DNA contents than the BLANK and BMP controls. Kucharska *et al.* [53] observed a similar trend in initial cell numbers when they cultured MG-63 osteoblast-like cells on chitosan-TCP microsphere based scaffolds. The cell numbers on the chitosan-TCP scaffolds were significantly lower than the controls 48 h post seeding; however, the elevated ALP activity of the cells at that time point suggested that the cells on the chitosan-TCP were being directed toward osteogenic differentiation as early as 2 days after seeding. Our ALP data at week 0 hint toward a similar phenomenon where rBMSCs were being directed toward osteogenic differentiation; however, no significant differences were observed in the ALP activities among groups at week 0. Although the DNA content was lower in the TCP/HAp groups initially, no significant differences were observed in DNA content among the study groups at later time points. The HYP and ALP results suggest that the incorporation of TCP and HAp in microsphere-based scaffolds enhanced synthesis of bone-relevant ECM components over time. The TCP/HAp groups at 6 weeks had roughly 8 times the amount of collagen per cell (HYP/DNA) as the BLANK and BMP controls, a trend we previously observed with HAp-only microsphere-based scaffolds with comparable HYP amounts compared to the HAp-only scaffolds [33]. In addition, the ALP activities in the TCP/HAp groups at week 6 were approximately 20 times higher than the activities in the BLANK and BMP groups at that time point. The total calcium content analysis suggests that the calcium detected in the TCP/HAp groups predominantly represented the inherent calcium remaining in these scaffolds. However, it was observed that the calcium content in the TCP/HAp 7:3 group at week 6 was about 1.4 times higher than the calcium content of its acellular equivalent. Additionally, the TCP/HAp 7:3 calcium content at week 6 was comparable to its week 3 value, indicating that the cells might have retarded microsphere degradation, perhaps by covering the microspheres with collagen, etc. Higher secretion of calcium by the cells or incorporation of inherent calcium into the newly synthesized might have also contributed to the observed differences in calcium content between the acellular and cellular scaffolds in the TCP/HAp 7:3 group.

Gene expression data highlighted some key differences in the differentiation of rBMSCs on TCP/HAp scaffolds compared to those on the BLANK and BMP scaffolds. The TCP/HAp groups compared to the BLANK and BMP controls had lower expression values for RUNX2, COL1A1, and IBSP expression early on and had higher expression values at later time points. These differences in the expression of TCP/HAP groups and controls indicated that the presence of TCP/HAp may have inhibited expression of osteogenic markers initially [33, 27]. On the other hand, elevated expression of osteogenic genes in the TCP/HAp groups at later time points signifies that the incorporation of ceramic mixture propelled the differentiation of the seeded cells toward osteogenic lineage. Furthermore, differences in gene expression were observed between the TCP/HAp encapsulating groups with both the groups showing fluctuating expressions for RUNX2, COL1A1, and BGLAP over time. These oscillating expression patterns in the TCP/HAp groups may suggest that the rBMSCs

responded differently to different TCP/HAp ratios in microsphere-based scaffolds [54, 30, 41, 31, 43].

Histological images of the engineered constructs at week 6 suggested higher cell numbers in the BLANK and BMP groups compared to the TCP/HAp groups. However, failure to observe any statistically significant differences in DNA content at week 6 among groups suggest that observed differences in cell number (if any) might have been due to differences in initial cell attachment. Masson's trichrome images pointed toward higher collagen synthesis in the TCP/HAp groups, thus agreeing with the biochemical results of the study that demonstrated higher collagen synthesis (on per cell basis) in TCP/HAp constructs at 6 weeks. Additionally, collagen I IHC images depicted that the TCP/HAp 1:1 scaffolds at week 6 stained more intensely for collagen I than the TCP/HAp 7:3 scaffolds, further concurring with the gene expression data where COL1A1 expression in TCP/HAp 1:1 scaffolds at week 6 was significantly higher than the TCP/HAp 1:1 group at that time point. Alizarin red and von Kossa stains demonstrated that all scaffold groups possessed a mineral matrix of calcium and calcium phosphates at week 6, with the TCP/HAp encapsulating groups exhibiting the most-intense staining. Additionally, the staining intensities for Alizarin red and von Kossa stains were higher in the TCP/HAp 7:3 group at week 6 than the intensities in the TCP/HAp 1:1 group at that time point. Furthermore, it was observed that the mineral staining intensities in the TCP/HAp 7:3 group at week 6 were higher than their acellular counterparts (Supplementary Figure 2). The TCP/HAp constructs are expected to stain positive for mineralization because of inherent mineral present in these scaffolds. The higher mineral staining intensities in the TCP/HAp 7:3 at week 6 suggest that the cells in the TCP/HAp 7:3 group either made more calcium or utilized inherent calcium as a raw material in the ECM, thereby agreeing with the calcium content results. Sudan Black staining indicated presence of residual polymer in all of the groups after 6 weeks of culture, although residual spherical shapes of the microspheres were evident only in the TCP/HAp groups. Additionally, the TCP/HAp scaffolds had a lower degree of swelling throughout the 6-week culture period than the BLANK and BMP scaffolds. The observance of intact microsphere structure with Sudan Black staining and less severity of the macroscopic changes in the TCP/HAp groups suggest that TCP and HAp encapsulation might have retarded polymer degradation due to their intrinsic buffering capacity [55].

In summary, the results of the current study demonstrated that TCP/HAp encapsulation into microsphere-based scaffolds altered microsphere morphology, impacted the mechanical properties of the scaffolds (i.e., reduced moduli) and influenced the differentiation of the seeded rBMSCs toward an osteogenic lineage. Higher end point ECM synthesis and enhanced expression of osteogenic markers in TCP/HAp groups relative to the BMP-2 group suggest that the TCP/HAp encapsulation fast-tracked the osteogenic commitment of cells on these scaffolds. Additionally, biochemical and gene expression evidence was presented for the TCP/HAp groups outperforming the BLANK and BMP controls. Furthermore, differences in gene expression profiles between the TCP/HAp groups hint that the cells responded differently to two different ratios of TCP and HAp presented to them. Lastly, we did not specifically explore degradation of the TCP/HAp scaffolds; however, our histological and macroscopic findings indicate that the presence of TCP/HAp altered polymer degradation in microsphere-based scaffolds [56, 57]. Altogether, it can be concluded that

TCP/HAp mixtures when incorporated into microsphere-based gradient scaffolds may be able to enhance the performance of the bone-like region of the engineered construct by providing raw materials for the regenerating tissue.

5. Conclusions

The current study employed bioceramic mixtures of TCP and HAp encapsulated in homogeneous microsphere-based scaffolds to promote osteogenesis of BMSCs. TCP/HAp mixtures boosted the secretion of extracellular matrix (ECM) components relevant to bone tissue and in some instances even outperformed the BMP-2 positive control group as indicated by the biochemical, gene expression, histology, and immunohistochemical data. Additionally, gene expression data hinted that the rBMSCs responded differently to different TCP/HAp ratios presented to them. Overall, it can be concluded that TCP/HAp mixtures when incorporated into microsphere-based gradient scaffolds may be able to enhance the performance of the bone-like region of the engineered construct by providing raw materials for the regenerating tissue.

Supplementary Material

Refer to Web version on PubMed Central for supplementary material.

Acknowledgments

This publication was supported by the National Institute of Arthritis and Musculoskeletal and Skin Diseases of the National Institutes of Health (R01 AR056347). The content is solely the responsibility of the authors and does not necessarily represent the official views of the National Institutes of Health. We would also like to recognize support from the Kansas Bioscience Authority Rising Star Award. In addition, we thank Prem Thapa for his assistance with SEM imaging and EDS mapping.

References

1. Di Luca A, Van Blitterswijk C, Moroni L. The osteochondral interface as a gradient tissue: From development to the fabrication of gradient scaffolds for regenerative medicine. Birth Defects Research Part C: Embryo Today: Reviews. 2015; 105(1):34–52.
2. Jeon JE, Vaquette C, Klein TJ, Hutmacher DW. Perspectives in Multiphasic Osteochondral Tissue Engineering. The Anatomical Record. 2013; 297(1):26–35. [PubMed: 24293311]
3. Lopa S, Madry H. Bioinspired Scaffolds for Osteochondral Regeneration. Tissue engineering Part A. 2014; 20(15–16):2052–2076. [PubMed: 24476065]
4. Renth AN, Detamore MS. Leveraging "raw materials" as building blocks and bioactive signals in regenerative medicine. Tissue Engineering Part B: Reviews. 2012; 18(5):341–362. [PubMed: 22462759]
5. Seo SJ, Mahapatra C, Singh RK, Knowles JC, Kim HW. Strategies for osteochondral repair: Focus on scaffolds. Journal of Tissue Engineering. 2014; 5(0):1–14.
6. Shimomura K, Moriguchi Y, Murawski CD, Yoshikawa H, Nakamura N. Osteochondral Tissue Engineering with Biphasic Scaffold: Current Strategies and Techniques. Tissue Engineering Part B: Reviews. 2014 140226120351005.
7. GĂśtz W, Lenz S, Reichert C, Henkel K, Pernicka L, Gundlach K, et al. A preliminary study in osteoinduction by a nano-crystalline hydroxyapatite in the mini pig. Folia histochemica et cytobiologica. 2011; 48(4):589–588.
8. Lü X, Wang J, Li B, Zhang Z, Zhao L. Gene expression profile study on osteoinductive effect of natural hydroxyapatite. Journal of Biomedical Materials Research Part A. 2014; 102(8):2833–2841. [PubMed: 24115491]

9. Fielding G, Bose S. SiO 2 and ZnO dopants in three-dimensionally printed tricalcium phosphate bone tissue engineering scaffolds enhance osteogenesis and angiogenesis in vivo. Acta biomaterialia. 2013; 9(11):9137–9148. [PubMed: 23871941]
10. Sungjin C. Implantation of tetrapod-shaped granular artificial bones or β-tricalcium phosphate granules in a canine large bone-defect model. The Journal of Veterinary Medical Science. 2014; 76(2):229. [PubMed: 24161964]
11. Bloemers FW, Blokhuis TJ, Patka P, Bakker FC, Wippermann BW, Haarman HJTM. Autologous bone versus calcium-phosphate ceramics in treatment of experimental bone defects. Journal of Biomedical Materials Research Part B: Applied Biomaterials. 2003; 66(2):526–531.
12. Fellah BH, Gauthier O, Weiss P, Chappard D, Layrolle P. Osteogenicity of biphasic calcium phosphate ceramics and bone autograft in a goat model. Biomaterials. 2008; 29(9):1177–1188. [PubMed: 18093645]
13. Yuan H, Fernandes H, Habibovic P, de Boer J, Barradas AM, de Ruiter A, et al. Osteoinductive ceramics as a synthetic alternative to autologous bone grafting. Proceedings of the National Academy of Sciences. 2010; 107(31):13614–13619.
14. Huang W, Li X, Shi X, Lai C. Microsphere based scaffolds for bone regenerative applications. Biomaterials Science. 2014; 2(9):1145–1153.
15. Berkland C, Kim K, Pack DW. Fabrication of PLG microspheres with precisely controlled and monodisperse size distributions. Journal of controlled release : official journal of the Controlled Release Society. 2001; 73(1):59–74. [PubMed: 11337060]
16. Blaker JJ, Knowles JC, Day RM. Novel fabrication techniques to produce microspheres by thermally induced phase separation for tissue engineering and drug delivery. Acta biomaterialia. 2008; 4(2):264–272. [PubMed: 18032120]
17. Borden M, Attawia M, Laurencin CT. The sintered microsphere matrix for bone tissue engineering: in vitro osteoconductivity studies. Journal of biomedical materials research. 2002; 61(3):421–429. [PubMed: 12115467]
18. Brown JL, Nair LS, Laurencin CT. Solvent/non-solvent sintering: a novel route to create porous microsphere scaffolds for tissue regeneration. Journal of biomedical materials research Part B, Applied biomaterials. 2008; 86(2):396–406.
19. Brown LR, Gombotz WR, Healy MS. inventors; US Patent Office, assignee. Very low temperature casting of controlled release microspheres. 1991
20. Nukavarapu SP, Kumbar SG, Brown JL, Krogman NR, Weikel AL, Hindenlang MD, et al. Polyphosphazene/nano-hydroxyapatite composite microsphere scaffolds for bone tissue engineering. Biomacromolecules. 2008; 9(7):1818–1825. [PubMed: 18517248]
21. Dormer NH, Busaidy K, Berkland CJ, Detamore MS. Osteochondral interface regeneration of rabbit mandibular condyle with bioactive signal gradients. Journal of Oral and Maxillofacial Surgery. 2011; 69(6):e50–e57. [PubMed: 21470747]
22. Dormer NH, Singh M, Wang L, Berkland CJ, Detamore MS. Osteochondral interface tissue engineering using macroscopic gradients of bioactive signals. Annals of biomedical engineering. 2010; 38(6):2167–2182. [PubMed: 20379780]
23. Dormer NH, Singh M, Zhao L, Mohan N, Berkland CJ, Detamore MS. Osteochondral interface regeneration of the rabbit knee with macroscopic gradients of bioactive signals. Journal of Biomedical Materials Research Part A. 2012; 100(1):162–170. [PubMed: 22009693]
24. Mohan N, Dormer NH, Caldwell KL, Key VH, Berkland CJ, Detamore MS. Continuous gradients of material composition and growth factors for effective regeneration of the osteochondral interface. Tissue engineering Part A. 2011; 17(21–22):2845–2855. [PubMed: 21815822]
25. Singh M, Dormer N, Salash JR, Christian JM, Moore DS, Berkland C, et al. Three-dimensional macroscopic scaffolds with a gradient in stiffness for functional regeneration of interfacial tissues. Journal of Biomedical Materials Research Part A. 2010; 94(3):870–876. [PubMed: 20336753]
26. Singh M, Morris CP, Ellis RJ, Detamore MS, Berkland C. Microsphere-based seamless scaffolds containing macroscopic gradients of encapsulated factors for tissue engineering. Tissue Engineering Part C-Methods. 2008; 14(4):299–309. [PubMed: 18795865]

27. Gupta V, Mohan N, Berkland CJ, Detamore MS. Microsphere-Based Scaffolds Carrying Opposing Gradients of Chondroitin Sulfate and Tricalcium Phosphate. Frontiers in Bioengineering and Biotechnology. 2015; 3:1–15. [PubMed: 25654078]
28. Mohan N, Gupta V, Sridharan BP, Mellott AJ, Easley JT, Palmer RH, et al. Microsphere-based gradient implants for osteochondral regeneration: a long-term study in sheep. Regenerative medicine. 2015; (0)
29. Chen Y, Wang J, Zhu XD, Tang ZR, Yang X, Tan YF, et al. Enhanced effect of β-tricalcium phosphate phase on neovascularization of porous calcium phosphate ceramics: in vitro and in vivo evidence. Acta biomaterialia. 2015; 11:435–448. [PubMed: 25246313]
30. Ebrahimi M, Pripatnanont P, Suttapreyasri S, Monmaturapoj N. In vitrobiocompatibility analysis of novel nano-biphasic calcium phosphate scaffolds in different composition ratios. Journal of biomedical materials research. 2013; 102(1):52–61. [PubMed: 23847019]
31. Imranul Alam M, Asahina I, Ohmamiuda K, Takahashi K, Yokota S, Enomoto S. Evaluation of ceramics composed of different hydroxyapatite to tricalcium phosphate ratios as carriers for rhBMP-2. Biomaterials. 2001; 22(12):1643–1651. [PubMed: 11374466]
32. Bhamidipati M, Sridharan B, Scurto AM, Detamore MS. Subcritical CO2 sintering of microspheres of different polymeric materials to fabricate scaffolds for tissue engineering. Materials Science and Engineering: C. 2013; 33(8):4892–4899. [PubMed: 24094202]
33. Dormer NH, Qiu Y, Lydick AM, Allen ND, Mohan N, Berkland CJ, et al. Osteogenic differentiation of human bone marrow stromal cells in hydroxyapatite-loaded microsphere-based scaffolds. Tissue Engineering Part A. 2011; 18(7–8):757–767. [PubMed: 21992088]
34. Jeon JH, Bhamidipati M, Sridharan B, Scurto AM, Berkland CJ, Detamore MS. Tailoring of processing parameters for sintering microsphere-based scaffolds with dense-phase carbon dioxide. Journal of biomedical materials research Part B, Applied biomaterials. 2013; 101(2):330–337.
35. Mohan N, Gupta V, Sridharan B, Sutherland A, Detamore MS. The potential of encapsulating “raw materials” in 3D osteochondral gradient scaffolds. Biotechnology and bioengineering. 2014; 111(4):829–841. [PubMed: 24293388]
36. Singh M, Sandhu B, Scurto A, Berkland C, Detamore MS. Microsphere-based scaffolds for cartilage tissue engineering: using subcritical CO(2) as a sintering agent. Acta biomaterialia. 2010; 6(1):137–143. [PubMed: 19660579]
37. Sridharan B, Mohan N, Berkland CJ, Detamore MS. Material characterization of microsphere-based scaffolds with encapsulated raw materials. Materials Science and Engineering: C. 2016; 63:422–428. [PubMed: 27040236]
38. Sutherland AJ, Detamore MS. Bioactive Microsphere-Based Scaffolds Containing Decellularized Cartilage. Macromolecular bioscience. 2015; 15(7):979–989. [PubMed: 25821206]
39. Singh M, Detamore MS. Stress Relaxation Behavior of Mandibular Condylar Cartilage Under High-Strain Compression. Journal of Biomechanical Engineering. 2009; 131(6):061008. [PubMed: 19449962]
40. Detamore MS, Athanasiou KA. Tensile Properties of the Porcine Temporomandibular Joint Disc. Journal of biomechanical engineering. 2003; 125(4):558–558. [PubMed: 12968581]
41. Ghanaati S, Barbeck M, Detsch R, Deisinger U, Hilbig U, Rausch V, et al. The chemical composition of synthetic bone substitutes influences tissue reactions in vivo: histological and histomorphometrical analysis of the cellular inflammatory response to hydroxyapatite, beta-tricalcium phosphate and biphasic calcium phosphate ceramics. Biomedical materials (Bristol, England). 2012; 7(1)
42. Hu J, Zhou Y, Huang L, Liu J, Lu H. Effect of nano-hydroxyapatite coating on the osteoinductivity of porous biphasic calcium phosphate ceramics. BMC musculoskeletal disorders. 2014; 15(1):114. [PubMed: 24690170]
43. Kurashina K, Kurita H, Wu Q, Ohtsuka A, Kobayashi H. Ectopic osteogenesis with biphasic ceramics of hydroxyapatite and tricalcium phosphate in rabbits. Biomaterials. 2002; 23(2):407–412. [PubMed: 11761160]
44. Sanda M, Shiota M, Fujii M, Kon K, Fujimori T, Kasugai S. Capability of new bone formation with a mixture of hydroxyapatite and beta-tricalcium phosphate granules. Clinical Oral Implants Research. 2014; 26(12):1369–1374. [PubMed: 25156136]

45. Schopper C, Ziya-Ghazvini F, Goriwoda W, Moser D, Wanschitz F, Spassova E, et al. HA/TCP compounding of a porous CaP biomaterial improves bone formation and scaffold degradation--a long-term histological study. Journal of biomedical materials research Part B, Applied biomaterials. 2005; 74(1):458–467.
46. Wongwitwichot P, Kaewsrichan J, Chua K, Ruszymah B. Comparison of TCP and TCP/HA hybrid scaffolds for osteoconductive activity. Open Biomedical Engineering Journal. 2010; 4:279–285. [PubMed: 21625376]
47. Bao T-Q, Franco R-A, Lee B-T. Preparation and characterization of novel poly(ε-caprolactone)/biphasic calcium phosphate hybrid composite microspheres. Journal of biomedical materials research. 2011; 98B(2):272–279.
48. Newbury DE. Mistakes encountered during automatic peak identification of minor and trace constituents in electron-excited energy dispersive X-ray microanalysis. Scanning. 2009; 31(3):91–101. [PubMed: 19533682]
49. Keaveny TM, Hayes WC. Mechanical properties of cortical and trabecular bone. Bone A treatise. 1993; 7:285–344.
50. Williams SK, Amiel D, Ball ST, Allen RT, Wong VW, Chen AC, et al. Prolonged storage effects on the articular cartilage of fresh human osteochondral allografts. The Journal of Bone and Joint Surgery (American). 2003; 85-A(11):2111–2120.
51. Moroni L, de Wijn JR, van Blitterswijk CA. 3D fiber-deposited scaffolds for tissue engineering: Influence of pores geometry and architecture on dynamic mechanical properties. Biomaterials. 2006; 27(7):974–985. doi:http://dx.doi.org/10.1016/j.biomaterials.2005.07.023. [PubMed: 16055183]
52. Sudarmadji N, Tan JY, Leong KF, Chua CK, Loh YT. Investigation of the mechanical properties and porosity relationships in selective laser-sintered polyhedral for functionally graded scaffolds. Acta Biomaterialia. 2011; 7(2):530–537. doi:http://dx.doi.org/10.1016/j.actbio.2010.09.024. [PubMed: 20883840]
53. Kucharska M, Walenko K, Lewandowska-Szumieł M, Brynk T, Jaroszewicz J, Ciach T. Chitosan and composite microsphere-based scaffold for bone tissue engineering: evaluation of tricalcium phosphate content influence on physical and biological properties. Journal of Materials Science: Materials in Medicine. 2015; 26(3):143–112. [PubMed: 25737128]
54. Arinzeh TL, Tran T, Mcalary J, Daculsi G. A comparative study of biphasic calcium phosphate ceramics for human mesenchymal stem-cell-induced bone formation. Biomaterials. 2005; 26(17):3631–3638. [PubMed: 15621253]
55. Agrawal CM, Athanasiou KA. Technique to control pH in vicinity of biodegrading PLA-PGA implants. Journal of biomedical materials research. 1997; 38(2):105–114. doi:10.1002/(SICI)1097-4636(199722)38:2<105::AID-JBM4>3.0.CO;2-U/asset/4_ftp.pdf. [PubMed: 9178737]
56. Niemelä T. Effect of β-tricalcium phosphate addition on the in vitro degradation of self-reinforced poly-l,d-lactide. Polymer Degradation and Stability. 2005; 89(3):492–500. doi:http://dx.doi.org/10.1016/j.polymdegradstab.2005.02.003.
57. Yang F, Cui W, Xiong Z, Liu L, Bei J, Wang S. Poly(l,l-lactide-co-glycolide)/tricalcium phosphate composite scaffold and its various changes during degradation in vitro. Polymer Degradation and Stability. 2006; 91(12):3065–3073. doi:http://dx.doi.org/10.1016/j.polymdegradstab.2006.08.008.

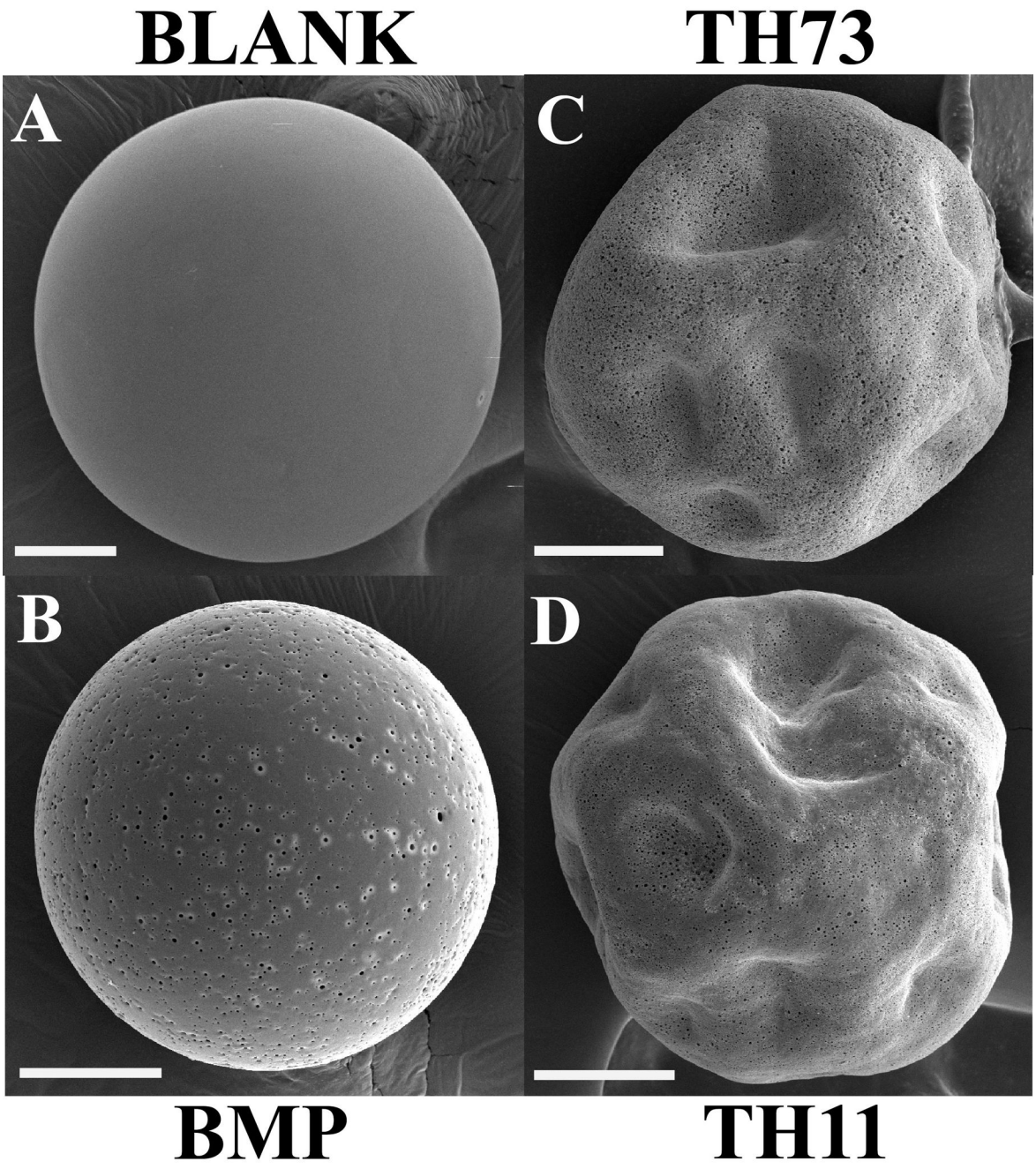

Figure 1.

Scanning electron micrographs of microspheres. BLANK (PLGA-only), BMP (PLGA with BMP-2 encapsulated), TH73 (PLGA with 30 wt% TCP/HAp 7:3), and TH11 (PLGA with 30 wt% TCP/HAp 1:1) microspheres. The images reveal the distinct morphological features of the microspheres used in different scaffold groups; note the porous nature of the surface of the BMP microspheres, and the deviation from the perfect spherical form for the TH73 and TH11 microspheres. Scale bars: 50 μm.

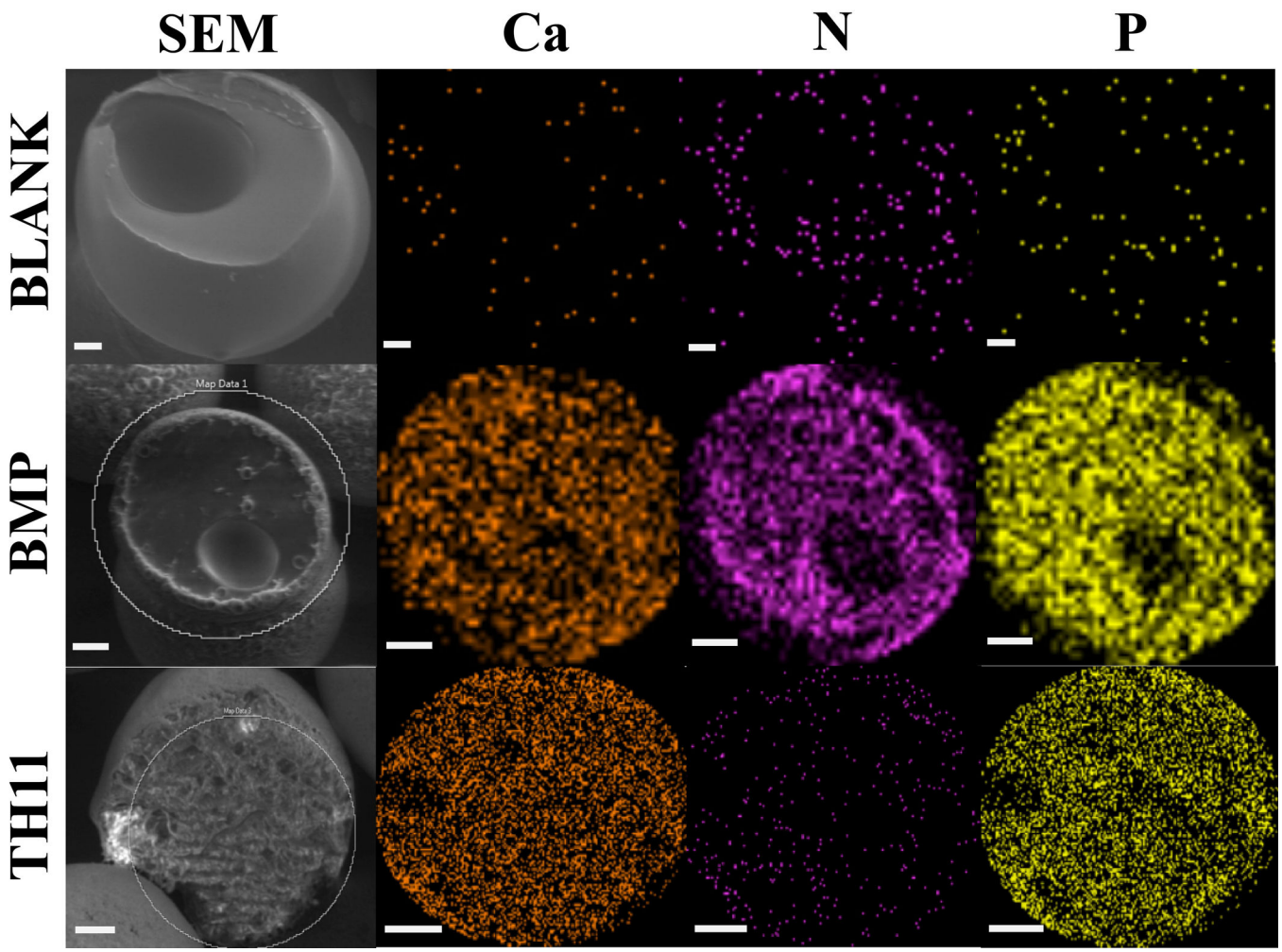

Figure 2.

Scanning electron micrographs (left column) and energy dispersive spectral maps of cryo-fractured microspheres for atomic calcium (Ca), nitrogen (N), and phosphorous (P). BLANK (PLGA-only), BMP (PLGA with BMP-2 encapsulated), and TH11 (PLGA with 30 wt% TCP/HAp 1:1). Note the uniform distribution of nitrogen in BMP microspheres and of calcium and phosphorus in the TH11 microspheres. Scale bars: 25 μm.

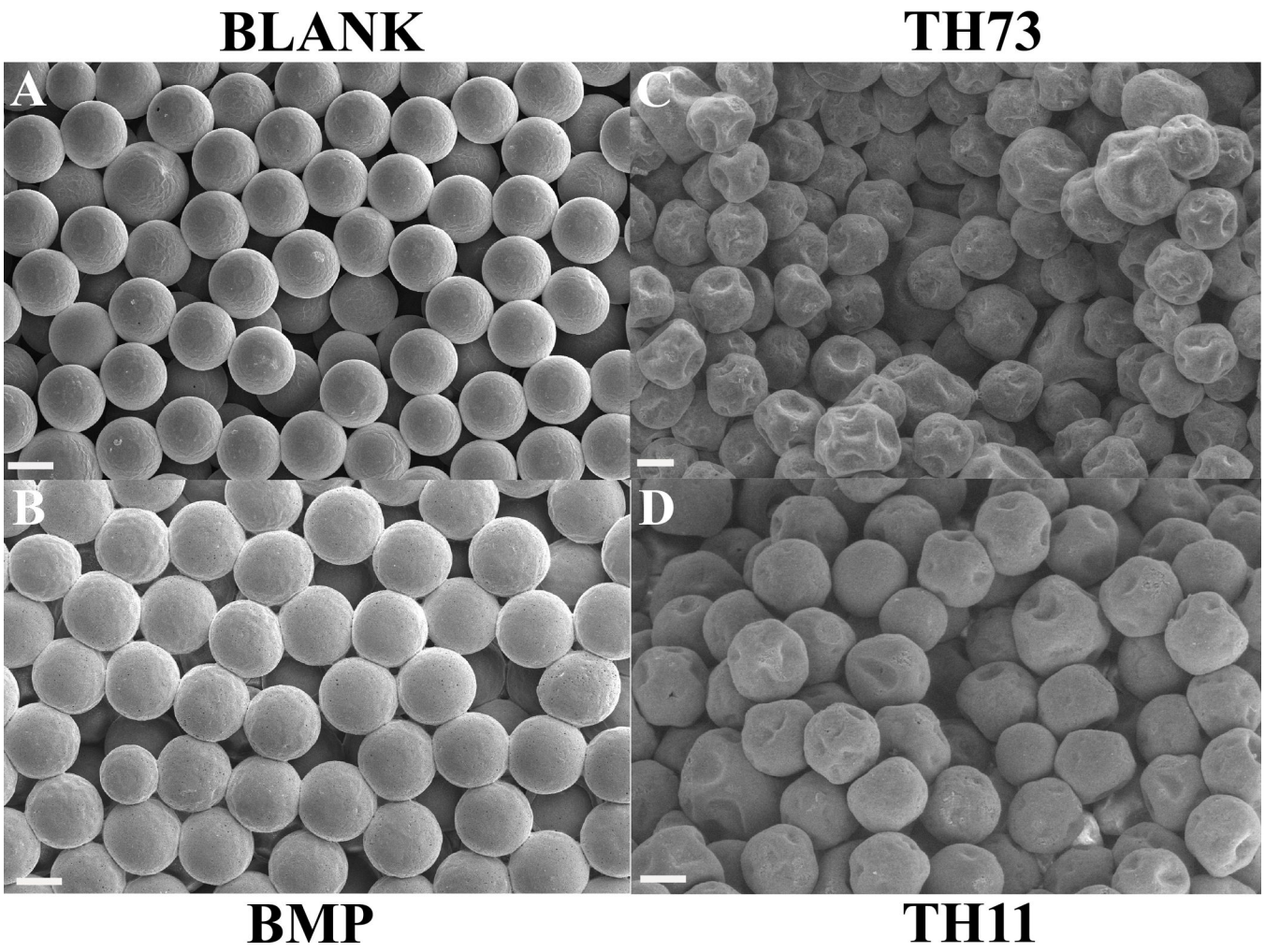

Figure 3.

Scanning electron micrographs of acellular microsphere-based scaffolds. BLANK (PLGA-only), BMP (PLGA with BMP-2 encapsulated), TH73 (PLGA with 30 wt% TCP/HAp 7:3), and TH11 (PLGA with 30 wt% TCP/HAp 1:1) scaffolds. All of the scaffolds were porous in nature with interconnected pores. Scale bars: 100 μm.

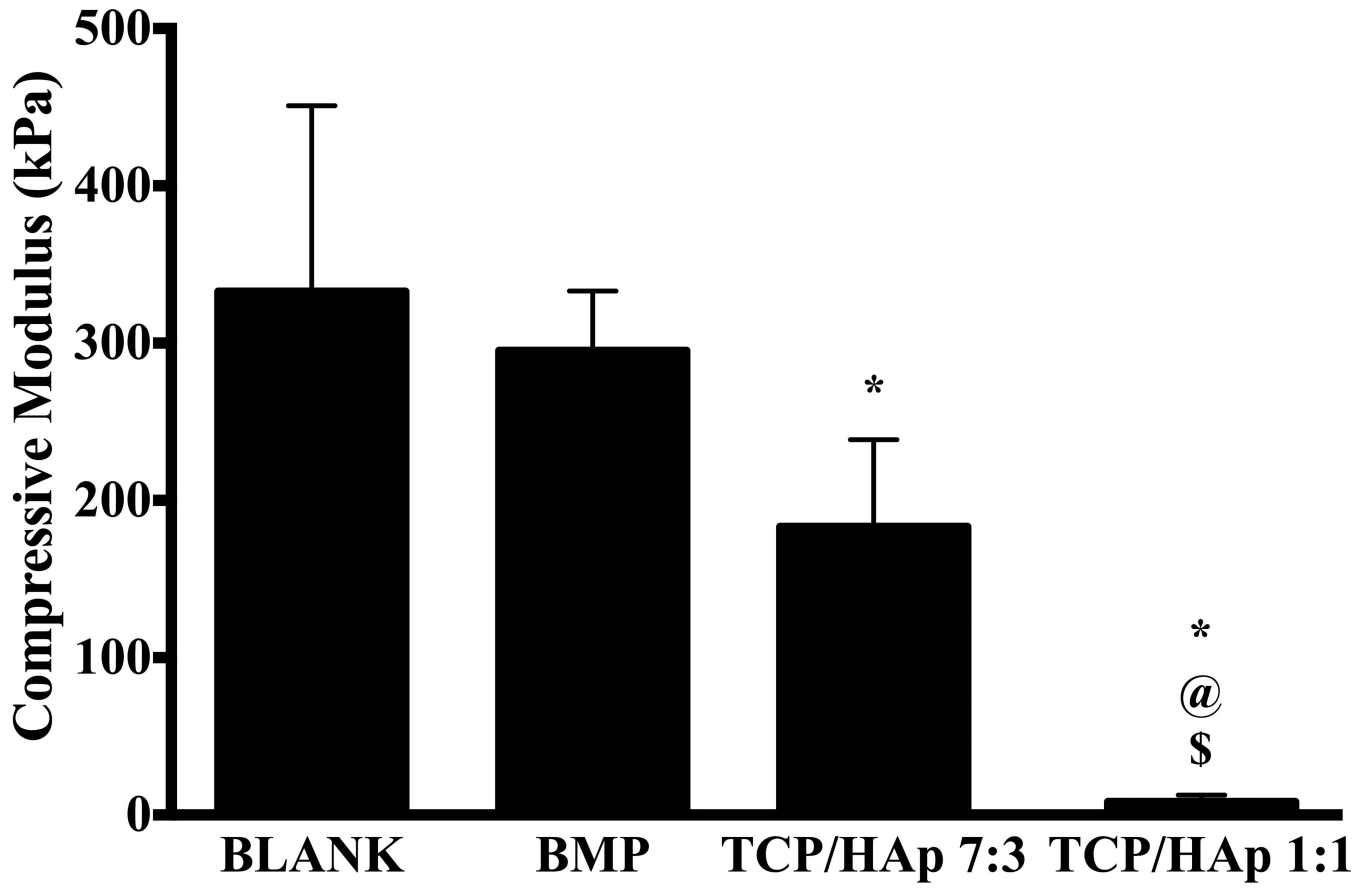

Figure 4.

Average compressive moduli of elasticity of acellular microsphere-based scaffolds at week 0. All values are expressed as the average + standard deviation (n = 6). The TCP/HAp groups had significantly lower moduli than the BLANK and BMP controls. *significant difference from the BLANK negative control group, @significant difference from the BMP positive control group, and $significant difference from the TCP/HAp 7:3 group ($p < 0.05$).

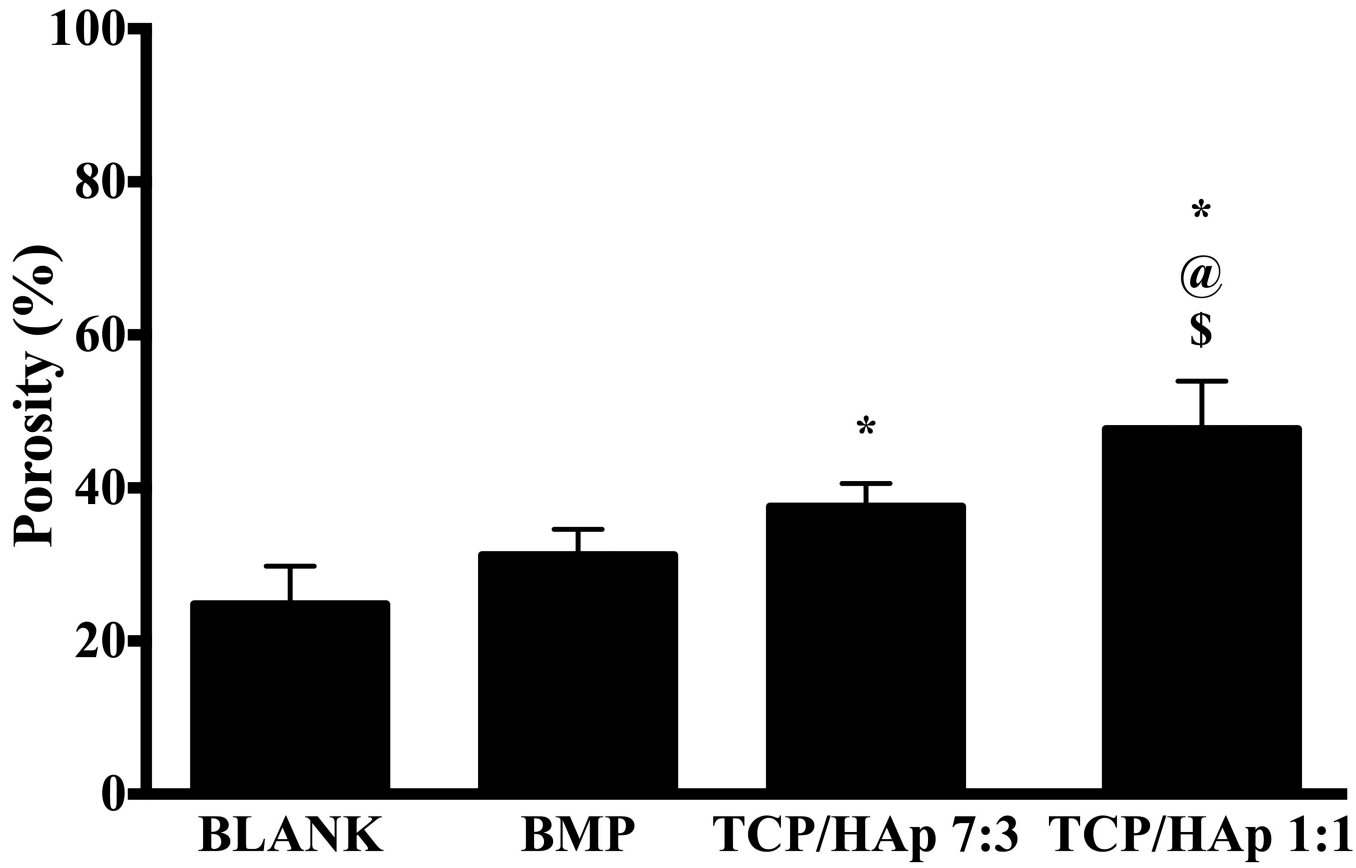

Figure 5.

Average porosities of different scaffold groups. All values are expressed as the average + standard deviation (n = 6). The TCP/HAp groups had significantly higher porosities than the BLANK and BMP controls. *significant difference from the BLANK negative control group, @significant difference from the BMP positive control group, and $significant difference from the TCP/HAp 7:3 group ($p < 0.05$).

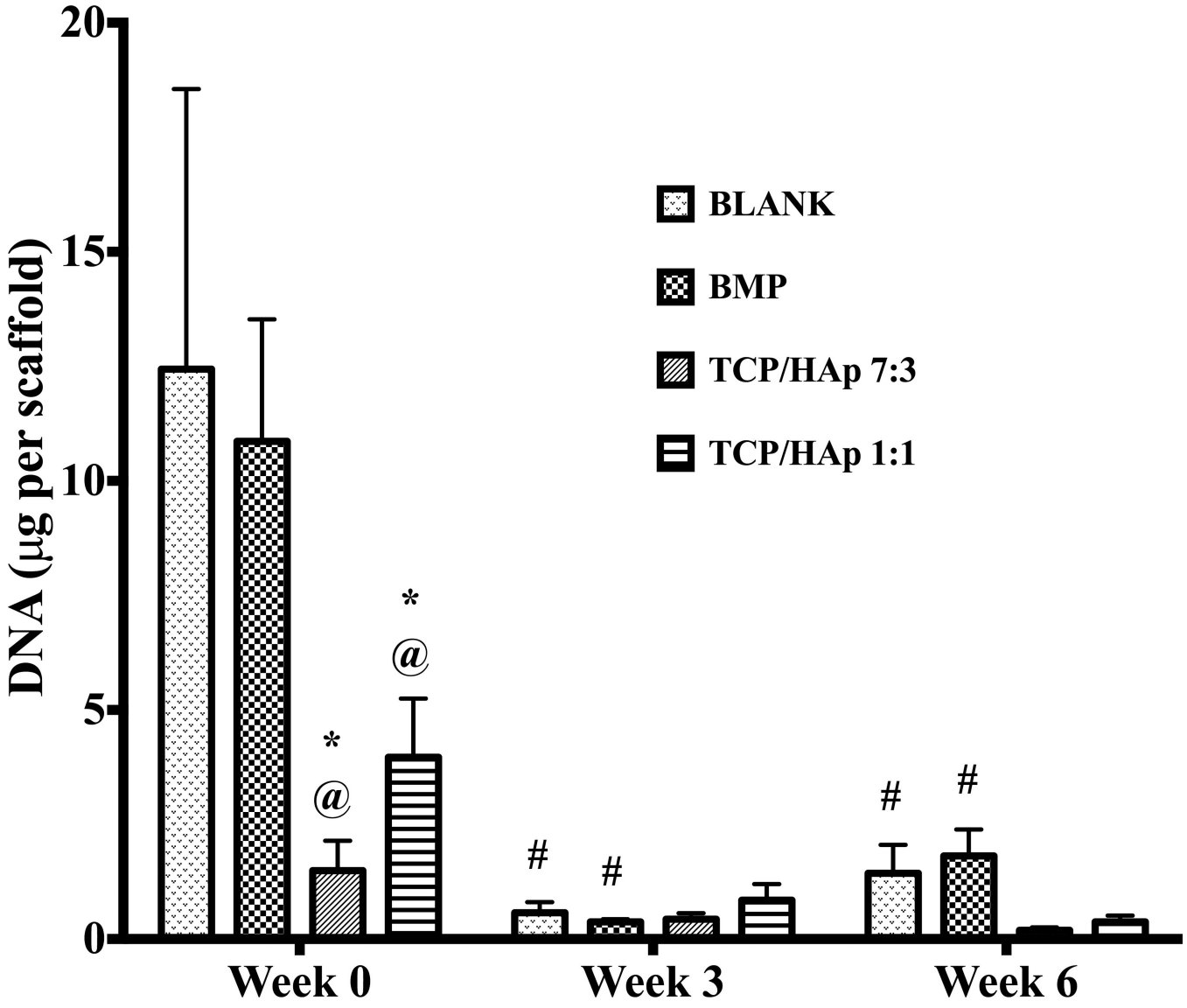

Figure 6.

Total DNA content as measured in the microsphere-based scaffolds over weeks 0, 3 and 6. All values are expressed as the average + standard deviation (n = 6). The TCP/HAp groups had significantly lower DNA content than the BLANK and BMP controls at week 0, while no significant differences were observed among the groups at later time points. *significant difference from the BLANK negative control group at same time point, @significant difference from the BMP positive control group at same time point, and #significant change from its value at week 0 ($p < 0.05$).

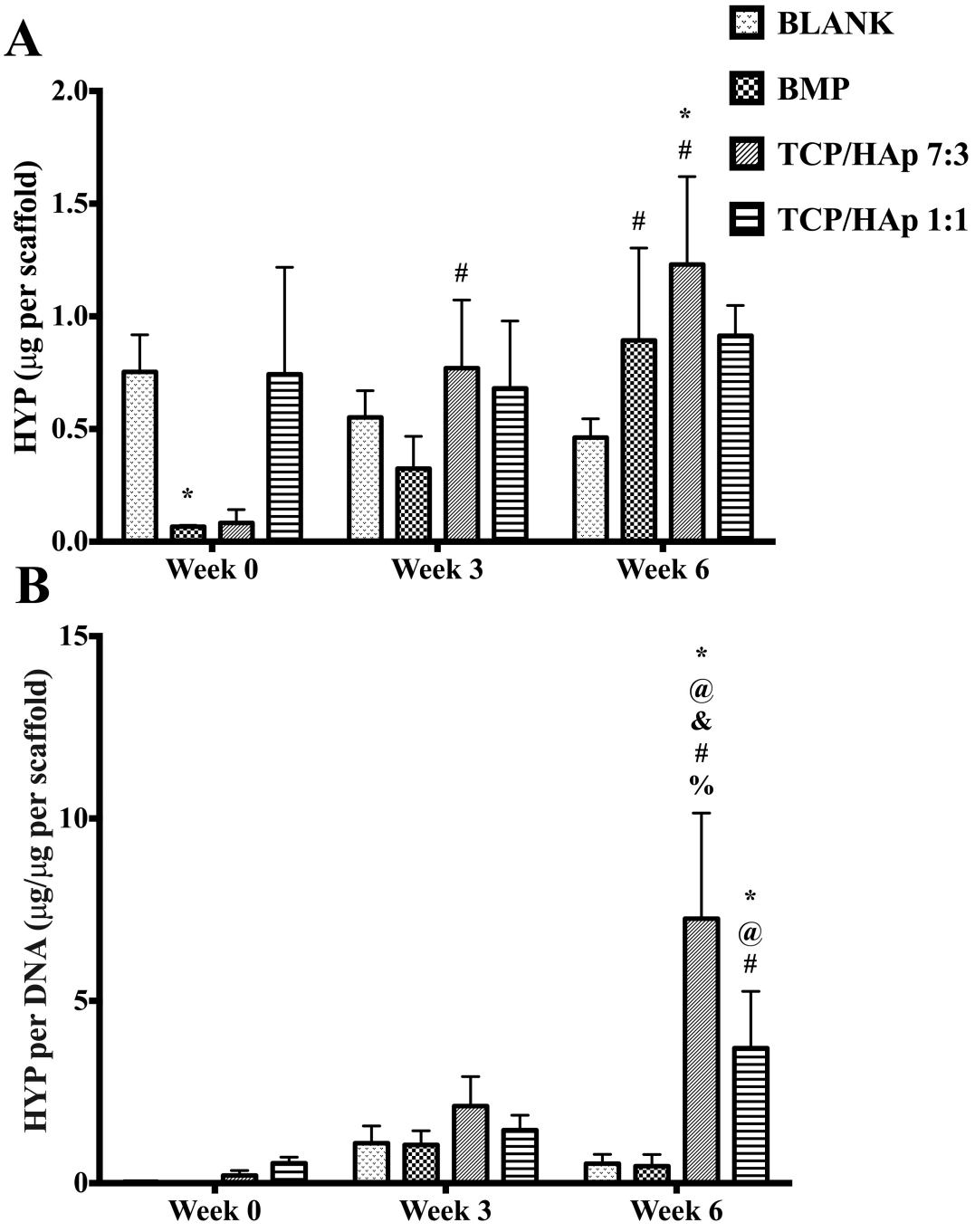

Figure 7.

HYP content as measured in the microsphere-based scaffolds over weeks 0, 3 and 6. (A) Total HYP content in micrograms per construct. (B) Normalized HYP content in micrograms per microgram of DNA. All values are expressed as the average + standard deviation (n = 6). The TCP/HAp groups had significantly higher normalized HYP content than the BLANK and BMP controls at week 6. *significant difference from the BLANK negative control group at same time point, @significant difference from the BMP positive control group at same time point, &significant difference from the TCP/HAp 1:1 group at

same time point, #significant change from its value at week 0, and %significant change from its value at week 3 ($p < 0.05$).

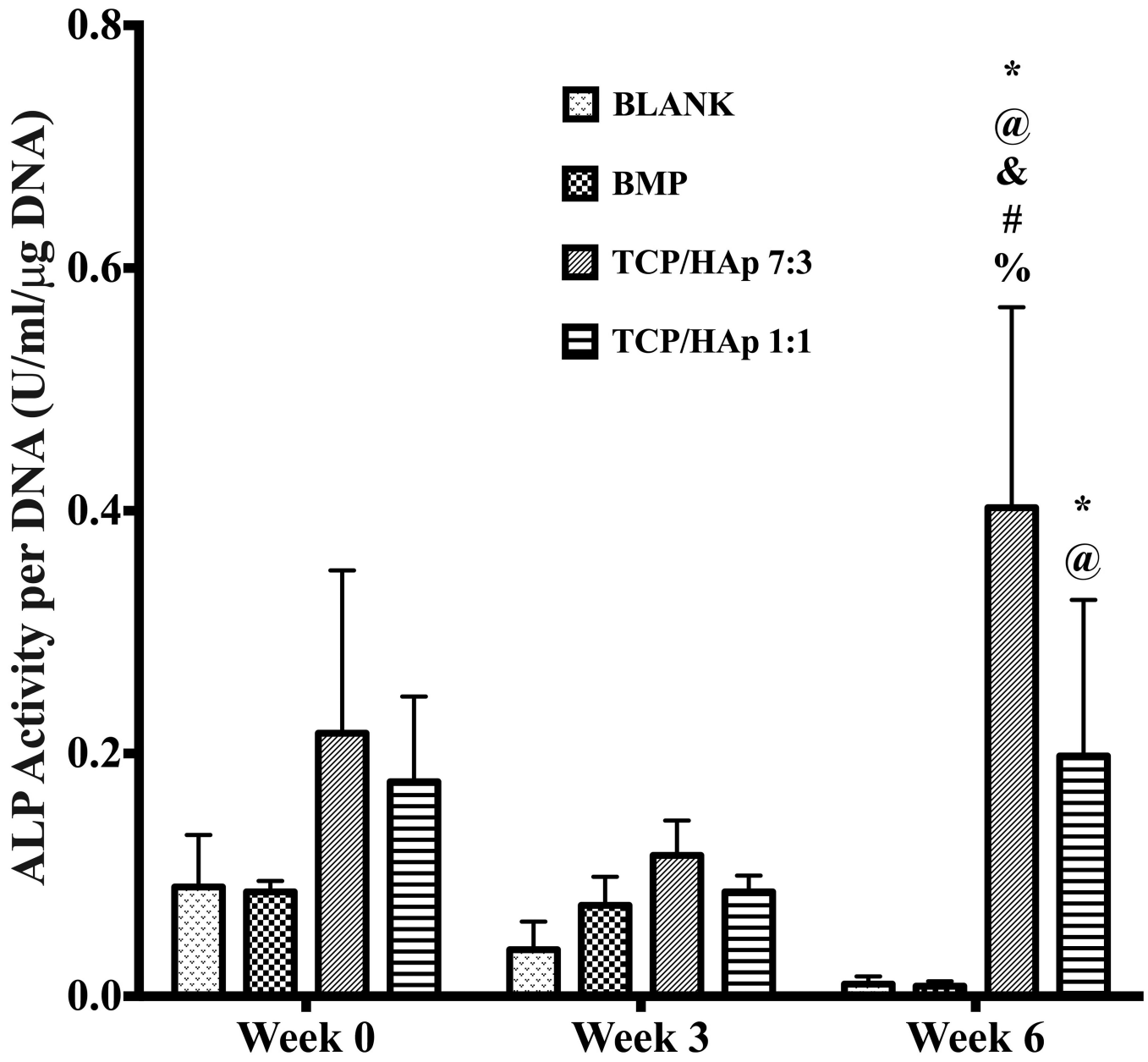

Figure 8.

ALP activity in 'Glycine Units' per micrograms DNA. Glycine Unit refers to the amount of enzyme causing the hydrolysis of one micromole of pNPP per minute at pH 9.6 and 25°C (glycine buffer). All values are expressed as the average + standard deviation (n = 6). The TCP/HAp groups outperformed the BLANK and BMP controls in ALP activity at week 6. *significant difference from the BLANK negative control group at same time point, @significant difference from the BMP positive control group at same time point, &significant difference from the TCP/HAp 1:1 group at same time point, #significant change from its value at week 0, and %significant change from its value at week 3 ($p < 0.05$).

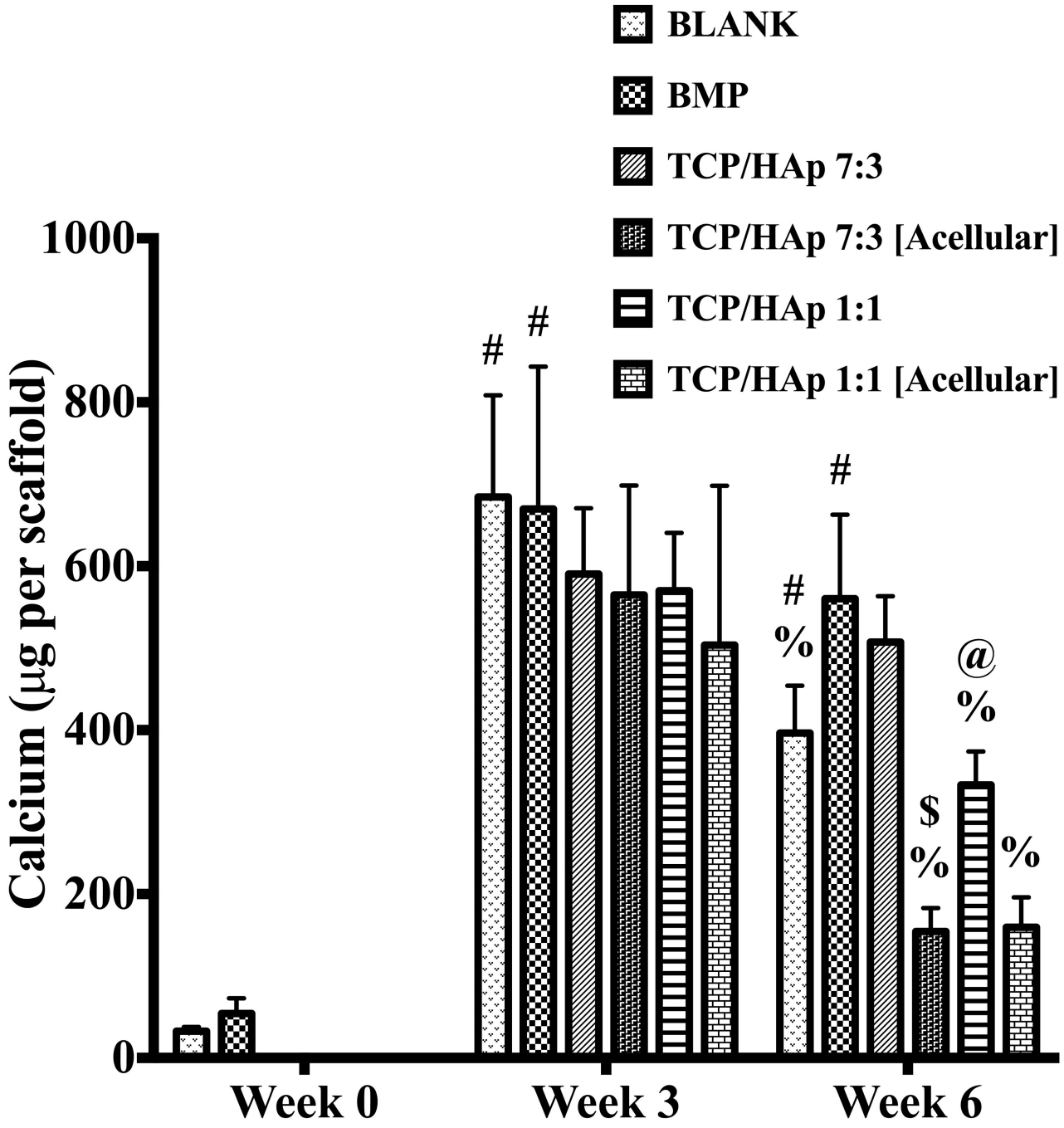

Figure 9.

Total calcium content as measured in the microsphere-based scaffolds over weeks 0, 3 and 6. The calcium contents of the TCP/HAp 7:3 and TCP/HAp 1:1 constructs (both cellular and acellular) at week 0 are not reported because of inadequate extraction of calcium from these scaffolds. All values are expressed as the average + standard deviation (n = 6). The TCP/HAp 7:3 group had significantly higher calcium than the TCP/HAp 7:3 [Acellular] group at week 6. @significant difference from the BMP positive control group at same time point, $significant difference from the TCP/HAp 7:3 group at same time point, #significant

change from its value at week 0, and %significant change from its value at week 3 ($p < 0.05$).

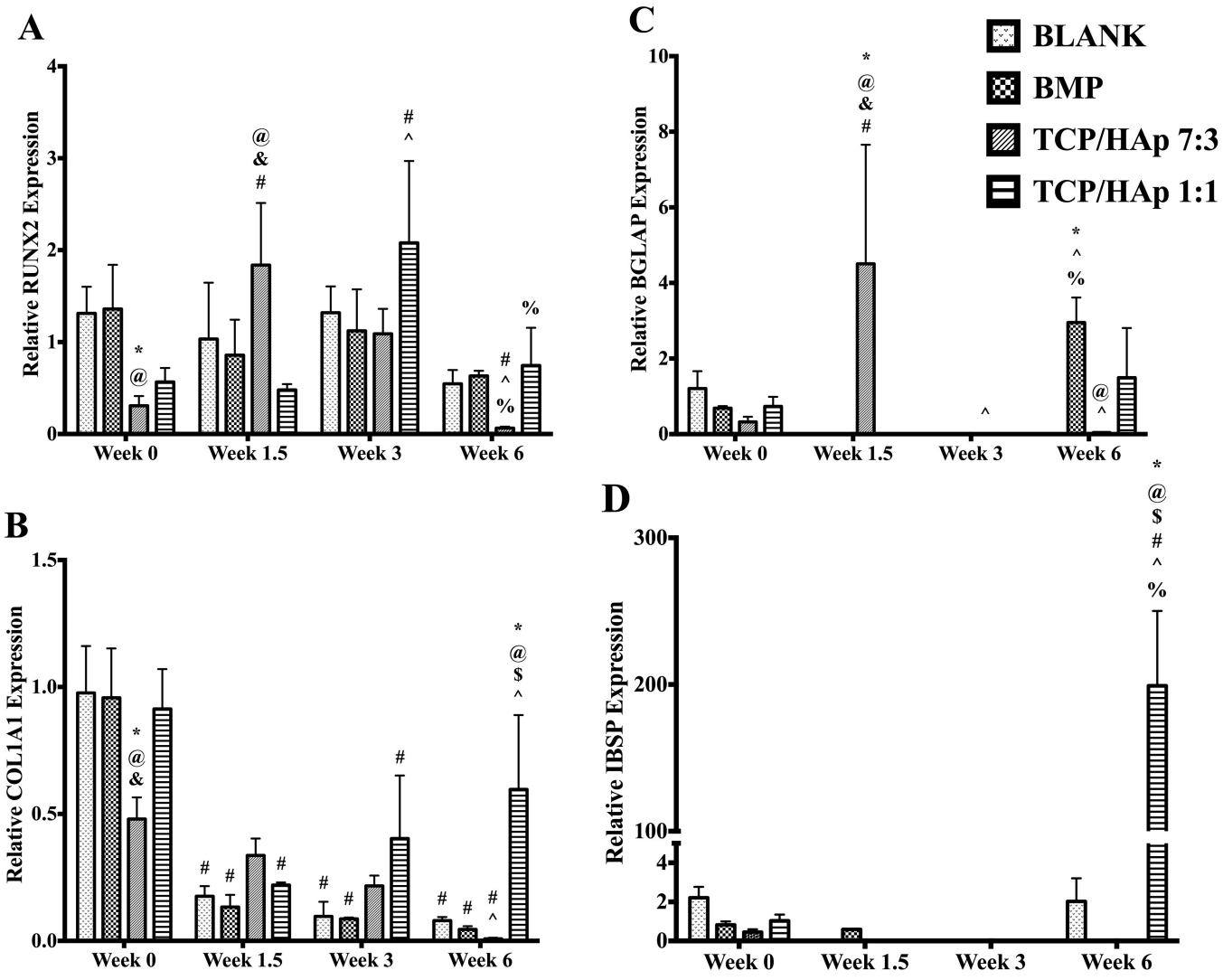

Figure 10.

Relative gene expression. All values are expressed as the average + standard deviation (n = 6). The gene expression of the TCP/HAp groups was lower compared to that of the BLANK and BMP controls initially; however, it was higher at later time points. *significant difference from the BLANK negative control group at same time point, @significant difference from the BMP positive control group at same time point, $significant difference from the TCP/HAp 7:3 group at same time point, & significant difference from the TCP/HAp 1:1 group at same time point, # significant change from its value at week 0, ^ significant change from its value at week 1.5, and % significant change from its value at week 3 ($p < 0.05$).

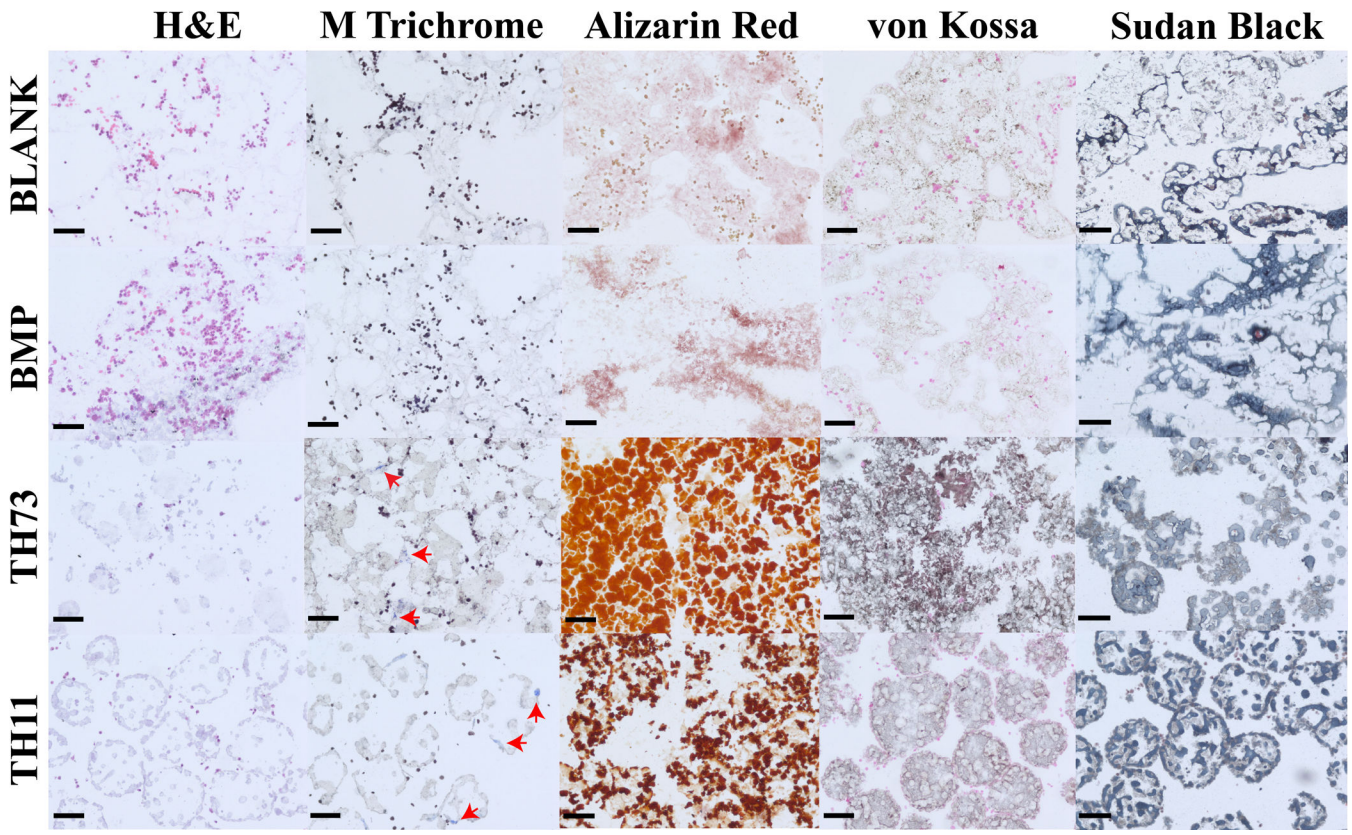

Figure 11.

Histological staining of cell-seeded microsphere-based constructs at week 6. BLANK, BMP, TH73 (TCP/HAp 7:3), and TH11 (TCP/HAp 1:1) scaffolds were stained for H&E, Masson's trichrome, Alizarin red, von Kossa, and Sudan Black. The TCP/HAp groups showed deposits of collagen (indicated by arrows), while no such deposits were observed in the BLANK and BMP controls. Scale bars: 100 μm.

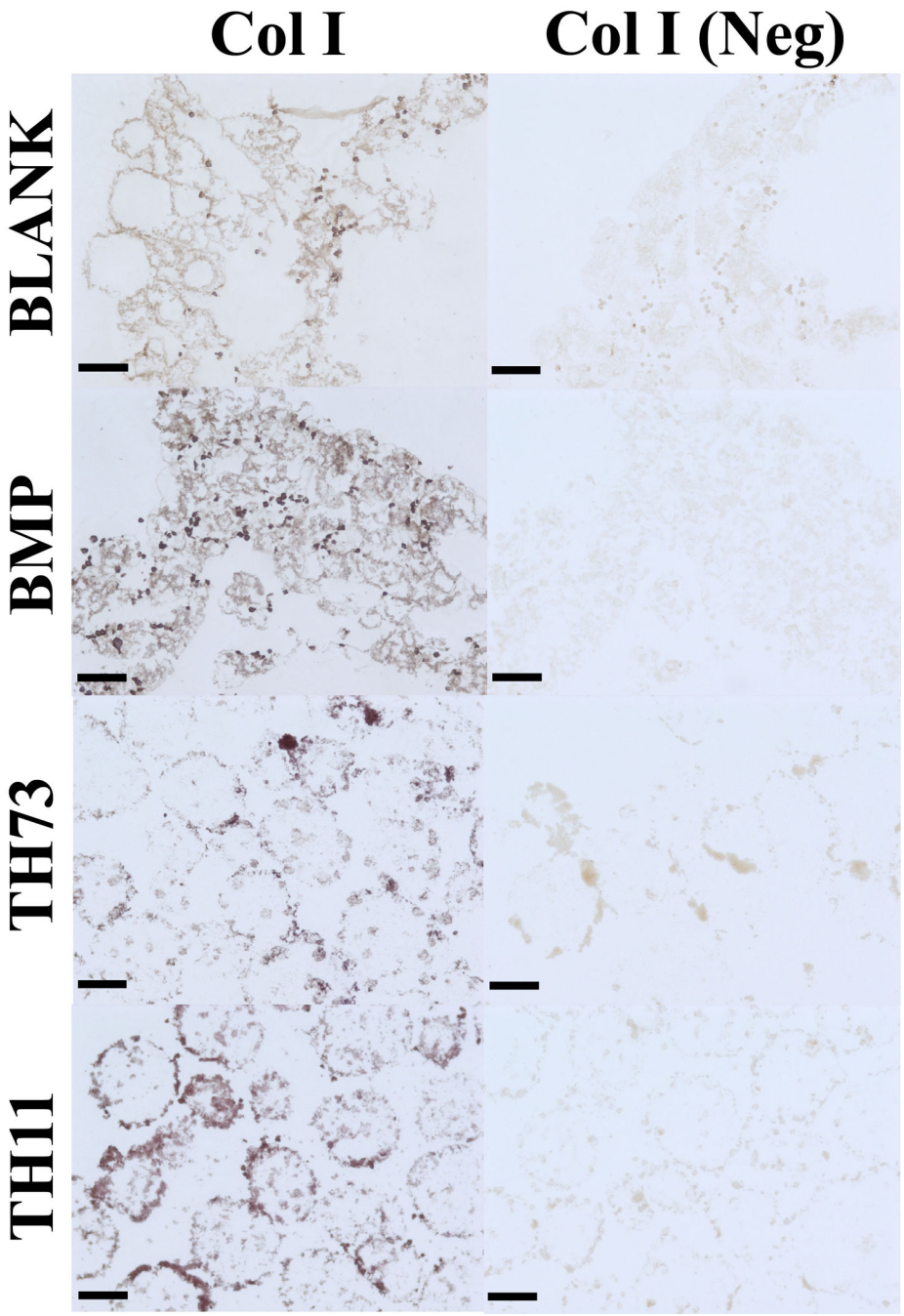

Figure 12.

Immunohistochemical staining of microsphere-based constructs at week 6. BLANK, BMP, TH73 (TCP/HAp 7:3), and TH11 (TCP/HAp 1:1) scaffolds were stained for Collagen I. Images of negative controls (primary antibody omitted) are also shown. Collagen I staining was more intense in the BMP and TCP/HAp 1:1 groups than the staining in the BLANK group. Scale bars: 100 μm.

Table 1

Genes used for RT-qPCR analysis

Gene	Symbol	TaqMan Assay ID
Glyceraldehyde 3-phosphate dehydrogenase	GAPDH	Rn01775763_g1
Collagen type I	COL1A1	Rn01463848_m1
Runt-related transcription factor 2	RUNX2	Rn01512298_m1
Bone gamma- carboxyglutamate protein	BGLAP	Rn00566386_g1
Integrin-binding sialoprotein	IBSP	Rn00561414_m1